Journal of Volcanology and Geothermal Research 452 (2024) 108139

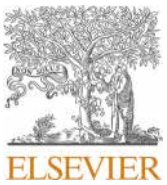

Contents lists available at ScienceDirect

Journal of Volcanology and Geothermal Research

journal homepage: www.journals.elsevier.com/journal-of-volcanology-and-geothermal-research

Investigating the potential influence of tectonic earthquakes on active volcanoes of Vanuatu

D. Legrand [a,*], P. Bani [b,c], S. Vergniolle [d]

[a] Universidad Nacional Autónoma de México, Instituto de Geofísica, Av. Universidad 3000, Coyoacán, C.P. 04510, Ciudad de México, Mexico
[b] Université Clermont Auvergne, CNRS, IRD, OPGC, Laboratoire Magmas et Volcans, F-63000 Clermont-Ferrand, France
[c] Antenne de Nouméa, Institut de Recherche pour le Développement (IRD), Nouvelle Calédonie, Nouméa, France
[d] Université Paris Cité, Institut de Physique du Globe de Paris, CNRS, F-75005 Paris, France

ARTICLE INFO

Keywords:
Earthquake triggering
Volcanic eruptions
Vanuatu volcanoes

ABSTRACT

It is intuitive to think that an earthquake near a volcano could disrupt its equilibrium and potentially trigger an eruption. But this cause-and-effect link is far from obvious for active volcanoes with an unknown internal stress state and the complexity of its magma-hydrothermal processes. This phenomenon is clearer in continental-oceanic subduction zones where volcanoes generally have closed-vent systems, differentiated high-viscosity magma, and active hydrothermal systems. This phenomenon is less well known in oceanic-oceanic subduction zones, where volcanoes often have open-vent systems, low-viscosity mafic magma, and hypothetic hydrothermal systems. The Vanuatu oceanic-oceanic subduction is an ideal zone to perform such study due to a high-seismic rate and volcanoes with different characteristics. The Vanuatu volcanoes display both open- and closed-vent systems, low and relatively high viscosity magma that enhance different types of volcanic activities (such as lava lakes, strombolian eruptions, high-eruptive columns, phreatic activity), and potential active hydrothermal systems. We compiled and identified sixty-nine cases of earthquakes potentially triggering volcanic activities on Vanuatu volcanoes from 1913 to 2018. Our findings indicate that the triggered volcanic responses occur co-seismically or shortly (at most 2–3 months later) after the earthquake, that the activated volcanoes are mainly located at near-field distances of the potentially triggering earthquake, implying a strong influence of static stress changes. Using the value of the seismic density energy, we suggest that the mechanism of the Vanuatu volcanic responses is due to changes of the permeability within active hydrothermal systems at Lopevi and Ambrym volcanoes in addition to the well-established ones, at Ambae, Garet, and Yasur volcanoes.

1. Introduction

Volcanoes and earthquakes in subduction zones are co-located, which raises the legitimate question of whether there is a cause-and-effect relationship between the two phenomena (Carr, 1977; Hill et al., 2002). However, the causal relationship between the occurrence of large earthquakes and volcanic activity is difficult to prove (Bebbington and Marzocchi, 2011; Sawi and Manga, 2018), especially in a subduction zone with high seismic and high volcanic activity. Over the last twenty years an increasing number of studies have emphasized, and statistically suggested, that a volcano can change its activity after the occurrence of a large earthquake (Darwin, 1840; Rockstroh, 1903; MacGregor, 1949; Blot, 1964, 1965; Latter, 1971; Yokoyama, 1971; Carr, 1977; Yamashina and Nakamura, 1978; Gudmundsson and Saemundsson, 1980; Blot, 1981; Sharp et al., 1981; Nercessian et al., 1991; Marzocchi et al., 1993; Barrientos, 1994; Walter and Amelung, 2007; Watt et al., 2009; Nishimura, 2017, 2021; Boulesteix et al., 2022). Statistical studies of this causal relationship require many observations, which is why they have been performed on a global scale using a catalogue of worldwide earthquakes and eruptions (Linde and Sacks, 1998; Marzocchi et al., 2002; Marzocchi, 2002; Manga and Brodsky, 2006; Eggert and Walter, 2009; Sawi and Manga, 2018). Marzocchi et al. (2002) showed a "statistically significant influence of distal strong earthquakes on the largest explosive eruptions of the 20th century. They model the interaction between earthquakes and eruptions in terms of the coseismic and postseismic stress diffusion. The stress variation consists of the elastic response of the lithosphere, and the viscoelastic relaxation of the asthenosphere and mantle, computed through a spherical,

* Corresponding author.
E-mail address: denis@geofisica.unam.mx (D. Legrand).

https://doi.org/10.1016/j.jvolgeores.2024.108139
Received 19 January 2024; Received in revised form 27 June 2024; Accepted 6 July 2024
Available online 8 July 2024

stratified, self-gravitating, viscoelastic Earth model. Their results show that the tectonic earthquakes induce on the volcanoes significant stress variations, from a few tenths to tens of bars, both in dilatation/compression and in shear stress … This indicates that the coseismic and postseismic stress diffusion might remotely induce eruptions, particularly for volcanoes close to a critical state". Marzocchi (2002) showed that there is a non-random correlation between large earthquakes and eruptions. He investigated whether "*the perturbation induced on a volcanic area by great tectonic earthquakes can modify the probability of a volcanic event. The results obtained showed that the occurrence of the largest explosive eruptions of the 20th century is significantly correlated to the earthquakes that occurred 0-5 and 30-35 years before, at distances up to 1000 km*". Manga and Brodsky (2006) found that "*approximately 0.4% of explosive volcanic eruptions occur within a few days of large, distant earthquakes. This many 'triggered' eruptions is much greater than expected by chance*". Linde and Sacks (1998) reached similar conclusions, supporting the idea of a statistical significance between large earthquakes and volcanic eruptions. Eggert and Walter (2009) conducted a review of "*previous works about the clustered occurrence of eruptions and earthquakes, and describe selected events. [They] further elaborated available databases and confirm a statistically significant relationship between volcanic eruptions and earthquakes on the global scale. Moreover, their study implies that closed volcanic systems in particular tend to be activated in association with a tectonic earthquake trigger. [They] then performed a statistical study at the subregional level, showing that certain subregions are especially predisposed to concurrent eruption-earthquake sequences, whereas such clustering is statistically less significant in other subregions*". Sawi and Manga (2018) conducted a comprehensive re-evaluation of the short-term impact of earthquakes on volcanic activity worldwide, analyzing data from a complete catalogue spanning 1964 to 2016. They found that ~4% of all the explosive eruptions (with a Volcanic Explosivity Index VEI $\geq$ 2, occurring shortly (within 5 days) after nearby ($<$ 800 km) earthquakes of magnitude $\geq$6) are potentially triggered eruptions. Nevertheless, they showed that this percentage increases to 5–12% when the time window is extended to 2 months to 2 years after large earthquakes, which is significantly larger than a random process.

Short-term reactivation (occurring within a few days of a potentially triggering earthquake) can be easily observed through changes in geophysical parameters such as seismic signals (Hill et al., 1993; Ukawa et al., 2002; Carniel et al., 2003; Moran et al., 2004; West et al., 2005; Pritchard et al., 2014; Hill and Prejean, 2015; Prejean and Hill, 2018), gas flux and composition (Cigolini et al., 2007; Avouris et al., 2017; Kennedy, 2017), heat flux (Harris and Ripepe, 2007; Delle Donne et al., 2010; Coppola et al., 2015), deformation (Pritchard et al., 2013, 2014; Takada and Fukushima, 2014; Shreve et al., 2021) and explosion rates (De la Cruz-Reyna et al., 2010; Coppola et al., 2015). Establishing such a causal relationship for a single volcano is more challenging, unless a complete and long-term dataset is available, as shown in the case of Popocatéptl volcano, Mexico, where periods of quiescence alternate with episodes of heightened seismic and volcanic activity (Boulesteix et al., 2022).

It has been shown statistically that large tectonic earthquakes are more likely to trigger eruptions in active subduction zones at partially plugged or closed-vent volcanoes, where fractionation promotes high-viscosity magma and emplacement of lava domes at the surface (Eggert and Walter, 2009; Bebbington and Marzocchi, 2011; Sawi and Manga, 2018). This is the case at some volcanoes in Chile (Eggert and Walter, 2009; Watt et al., 2009), Indonesia (Bebbington and Marzocchi, 2011) and México with the Popocatépetl volcano (Boulesteix et al., 2022). It has been proposed that partially plugged or closed-vent systems release less gas, with a decrease exceeding 20% after triggering earthquakes (Avouris et al., 2017), due to an elastic response that seals cracks, thus reducing the gas flow (Heap and Kennedy, 2016; Avouris et al., 2017; Campion et al., 2018). Cracks can also close during or after the passage of seismic waves generating dynamic or static stresses. Consequently, for these volcanoes, an earthquake can promote pressure build-up in the conduit, potentially triggering an eruption (Kennedy, 2017). On other volcanic systems, sustained by less differentiated magmas with open-vent manifestations, the cause-and-effect relationship with earthquake is even less obvious, although a 20% of SO_2 mass was observed above persistently degassing volcanoes following a list of 69 large earthquakes ($M_w \geq 7$) recorded between 2004 and 2010 (Avouris et al., 2017).

The reason why a volcanic activity sometimes occurs after potential triggering earthquakes is yet to be fully characterized and understood, however it is generally attributed to stress-field changes induced by the earthquake (Linde and Sacks, 1998; Hill et al., 2002; Kilb et al., 2002; Manga and Brodsky, 2006; Hill and Prejean, 2015; Nishimura, 2017). An earthquake generates seismic waves composed of a dynamic part followed by a static part. The dynamic part is mainly composed of the P waves, the near-field waves, the S waves, the Love and Rayleigh waves listed in order of their arrival times. The displacement amplitudes of the P and S waves decay as $1/r$ (where r is the distance), the displacement amplitudes of the near-field waves decay as $1/r^2$, and the displacement amplitudes of the surface Love and Rayleigh waves decay with a law varying from $1/r^{1.66}$ to $1/r$ (Johnson, 1974; Lay and Wallace, 1995; Legrand and Delouis, 1999; Aki and Richards, 2002; Shearer, 2009). The static part corresponds to the permanent ground displacement around the offset of the fault, which is a wave of frequency zero. The displacement amplitude of the static part decays as $1/r^2$. Hence the near-field waves and the static displacement field decay as $1/r^2$, more rapidly than the far-field P and S body waves, than the far-field surface waves, and are well recorded at near-field distances. The far-field P, S and surface waves are well recorded both at far-field and near-field distances. An important question is to know the limit between the near-field and far-field distances. Therefore, it is important to know until which distances the near-field waves are recorded. It is classically said that this distance is about one (or two) rupture fault length(s) (Wells and Coppersmith, 1994). Nevertheless Vidale et al. (1995), Cummins (1997), and Aki and Richards (2002) extended this distance to 10 time the rupture fault length because they showed that near-field waves were recorded at such large distances using broad-band seismometers. Zhang et al. (2023) also considered a factor of 10 between the length of the rupture fault and the epicentral distance in the case of far-field water-level co-seismic response. Hence, at near-field distances, the near-field waves and the static displacement field are dominant, whereas at far-field distances, only the far-field dynamic waves have a significant amplitude, even if far-field waves also propagate at near-field distances. These dynamic and static seismic waves generate dynamic and static stress fields, respectively.

The permanent static-stress can act over a long-time scale (Tokarev, 1971; Nakamura, 1975a, 1975b; Rikitake and Sato, 1989; Linde and Sacks, 1998; Díez et al., 2005; Walter, 2007; Walter et al., 2007). This may explain the long-time delays (from days, months to years) in some earthquake-triggering eruptions (Rojstaczer et al., 1995; Marzocchi, 2002; Watt et al., 2009; Chesley et al., 2012; Bonali, 2013). These static stress changes, when they are dilatational below the volcano, generate a volumetric expansion of the magma reservoir, favoring the growth of bubbles, and vertical motions of magma towards the surface (Barrientos, 1994; Hill et al., 2002; Walter and Amelung, 2007; Nishimura, 2021).

The dynamic stress can induce nucleation and bubble growth within the magma chamber (Linde and Sacks, 1998; Hill et al., 2002; Manga and Brodsky, 2006; Walter et al., 2007; Bonali et al., 2013; Hill and Prejean, 2015) causing liquefaction of the crystalline mush (Sumita and Manga, 2008) or oscillation of bubbly magma (sloshing) generating the collapse of magmatic foams, releasing gas, and initiating eruptions (Namiki et al., 2016).

The amplitude of the stress changes produced by an earthquake depends on the magnitude and distance of the earthquake (Mogi et al., 1989; Roeloffs, 1998; King et al., 1999; Manga and Brodsky, 2006; Wang et al., 2006; Wang, 2007). To take into account these two informations into a single parameter, a nondimensional index can be used which is the

ratio d/$\sqrt{S}$ of the earthquake-volcano epicentral distance (d) and the characteristic length of the earthquake ($\sqrt{S}$: square root of the rupture surface S), called the potential triggering index TRIGI by Legrand (2022). A small value of this dimensionless distance, TRIGI≤10, corresponds to a near-field earthquake-volcano epicentral distance, whereas a large value (TRIGI >10) corresponds to a far-field distance (Vidale et al., 1995; Aki and Richards, 2002; Zhang et al., 2023). The parameter TRIGI is very simple and is usefull to define the limit between the near- and the far-field. Alone it is insufficient to fully characterize the shaking of an earthquake, because the same value of TRIGI can result in different values of shake velocity, acceleration or strain. A small TRIGI value is neither a prove of cause-and-effect relationship between the occurrence of an earthquake and the reactivation of a volcano, it just evaluates the potential impact of an earthquake, with a given magnitude and distance, on a volcano. Similar approach was used by Kuribayashi and Tatsuoka (1975); Manga and Brodsky (2006); Manga and Wang (2007); Wang (2007) who plotted the distance between an earthquake of magnitude "M" and the location of soil liquefaction that occurred after the earthquake. They deduced a maximum distance of liquefaction depending on the magnitude "M". Wang and Manga (2010) extended the triggering effects for other hydrologic changes such as mud volcanoes, stream flows, magmatic volcanic eruptions, well level, hot spring, triggered earthquakes and geysers.

To further constrain the cause-effect relationship between a potentially triggering earthquake and a volcanic activity, we focused in this work on Vanuatu arc. We first compiled a list of earthquakes in the literature that were reported to potentially trigger a volcanic activity and calculated their corresponding TRIGI values. We completed this list with the largest eruptions (VEI ≥ 3) not associated to earthquakes in the literature for which we calculated the TRIGI values, and we compared them to the cases found in the literature. We finally suggested that the change of the volcanic activity to a potentially triggering earthquake may be due to the change of the permeability in active hydrothermal systems on the Vanuatu volcanoes.

2. Geological setting

The Vanuatu (ex New Hebrides) island-Arc is a seismically and volcanically active region located in the south-west Pacific, resulting from the convergence between the Australian plate and the North Fiji Basin, and is considered as an intra-oceanic arc. Convergence velocity directions to the trench are almost perpendicular to the trench throughout the NNW-SSE arc, even in its southernmost part (22°S-24°S) where the trench turns *E*-W (Louat and Pelletier, 1989). The relative convergence velocities are among the highest in the world, varying from 9 to 16 cm/yr, except in the central (between 15°S and 17°S) and the southernmost (south of 22°S) parts where they are reduced and vary between ~3 and ~ 5 cm/yr (Pelletier et al., 1998; Calmant et al., 2003; Bergeot et al., 2009; Baillard et al., 2018). At these two low-velocity places, the subduction-collision of the d'Entrecasteaux and the Loyalty ridges, in the central and southern parts of the subduction zone respectively, lead to a lack of trench and produce transverse fault systems and even compression in the arc and back-arc zone, east of the Ambae, Ambrym and Lopevi volcanoes (Collot et al., 1985; Louat and Pelletier, 1989; Taylor et al., 1995; Lagabrielle et al., 2003), as well as the transform fault across the arc in the front of the Loyalty ridge (Louat and Pelletier, 1989).

The rate of seismicity along the Vanuatu arc is high, approximatively 260 earthquakes of magnitudes 7+ (i.e., >2 per year), among which eight are of magnitude 7.9+ (~6.6 each 100 years), between 1900 and 2022. The largest recorded earthquakes occurred on 14 October 1913 (of magnitudes M8.1 defined by Linde and Sacks (1998) and 7.6 by Engdahl and Villaseñor, 2002, on 20 September 1920 (M8.09 ± 0.41, re-calculated by the USGS in 2022), although re-estimated between 7.5 and 7.8 by Ioualalen et al. (2017) and M7.8 by Engdahl and Villaseñor (2002), on 6 February 2013 (M8.0), 9 August 1901, 2 December 1950, 31 December 1966, 17 July 1980, 21 April 1997 (M7.9), 16 June 1910, 17 December 1957, 7 October 2009 (M7.8), the 18 July 1934, 20 May 1965, 16 May 1995, 10 February 2021, 19 May 2023 (M7.7). The depths of historic earthquakes are difficult to calculate or estimate. One way to constrain the depth more reliably is to compare the old earthquake with more recent earthquakes of similar epicenters, based on the hypothesis that earthquakes of similar epicenters in a subduction zone will have similar depths. For example, the earthquake, which occurred on 20 May 1965, is an intermediate-depth (120 km) event if we consider the depth given by the USGS but is a shallow-depth (10 km) earthquake if we consider Engdahl and Villaseñor (2002). We prefer the estimate of 120 km depth for the 1965 earthquake when comparing with recent (1980–2023) and nearby epicenter earthquakes of magnitudes ≥6.0, which have better depth determinations. The 1910 and 1913 earthquakes are intermediate and deep earthquakes with depths at 100 km and 230 km respectively defined by Engdahl and Villaseñor (2002). If we compare the recent earthquakes of similar epicenters with magnitudes ≥6.0 to that of the 1910 epicenter, its depths can either be of the order of 20 km or ~ 120–130 km. Hence the depth of the 1910 is not well constrained. The nearby recent earthquakes close to the 1913 earthquake have depths of ~110–120 km so shallower than the value proposed for the 1913 earthquake, 230 km (Engdahl and Villaseñor (2002)). Most of the magnitude 7.7+ earthquakes are located in the northern and southernmost parts of the Vanuatu subduction zone (Fig. 1). Two seismic gaps can be identified. One is included in the region between ~13°S and ~ 18°S (if we excluded the deep 1910, 1913, and 1965 intra-slab earthquakes). Another one is included in the region between ~18°S and 23°S if we exclude the oldest and deeper 1901, 1910, 1913 and 1920 earthquakes (Fig. 1).

3. Description of Vanuatu volcanoes

The active volcanoes present in the Vanuatu volcanic island arc include Ambae (Aoba), Ambrym, East-Epi (submarine volcano), Karua (submarine volcano in the Kuwae caldera), Lopevi, Mount Garet (Gaua), Suretamatai, and Yasur (Tanna) (MacFarlane et al., 1988; Peate et al., 1997; Vergniolle and Métrich, 2016, 2022).

The Vanuatu volcanoes belong to both, open- and closed-vent types. The definition of open-vent or closed-vent system is not completely consensual and differs depending on what is observed: the SO_2 gas flux, the presence of magma exposed to the surface, thermal anomalies, acoustic signals, presence of a plug/dome at the top of the magma conduit etc.… Moreover, the open- or closed- character can change with time during the life of a volcano, so a volcano is not always a closed-vent system or always an open-vent system. Here we use the following definition based on the conduit itself: an open-vent system corresponds to the conduit that is physically opened and thus shows magma exposed to the surface, whereas a closed-vent system does not have magma exposed to the surface thus does not show a persistent and visible magmatic activity. Thus, this definition is independent of the gas flux. The magma of the Vanuatu volcanoes are known for their diversity, ranging from the typical basalts to the basaltic trachyandesite or felsic andesites for the most differentiated magma. Eruptive patterns at Vanuatu volcanoes vary from one volcano to another and they can also change for a same volcano. It can be a typical lava lake activity (Ambrym), strombolian to vulcanian activity (Yasur), eruptive columns reaching a height of a few km to >10 km (Lopevi, Garet, Ambae), and phreatic explosions (Ambae, Mont Garet). The main characteristics of the five largest area and active Vanuatu volcanoes (Fig. 2) are described below (classified in the alphabetic order).

The 38 km × 16 km Ambae island (also named Aoba) is the emerged part of a large basaltic volcano of 3900 m high from seabed (with an emerged part of 1496 m above sea level) hosting three lakes including the warm acidic crater lake Voui, one of the largest (~2 km^2) crater lake worldwide (before the 2017–2018 eruption), Manaro Lakua (Warden, 1970; Robin and Monzier, 1994) and a third small one named Manaro

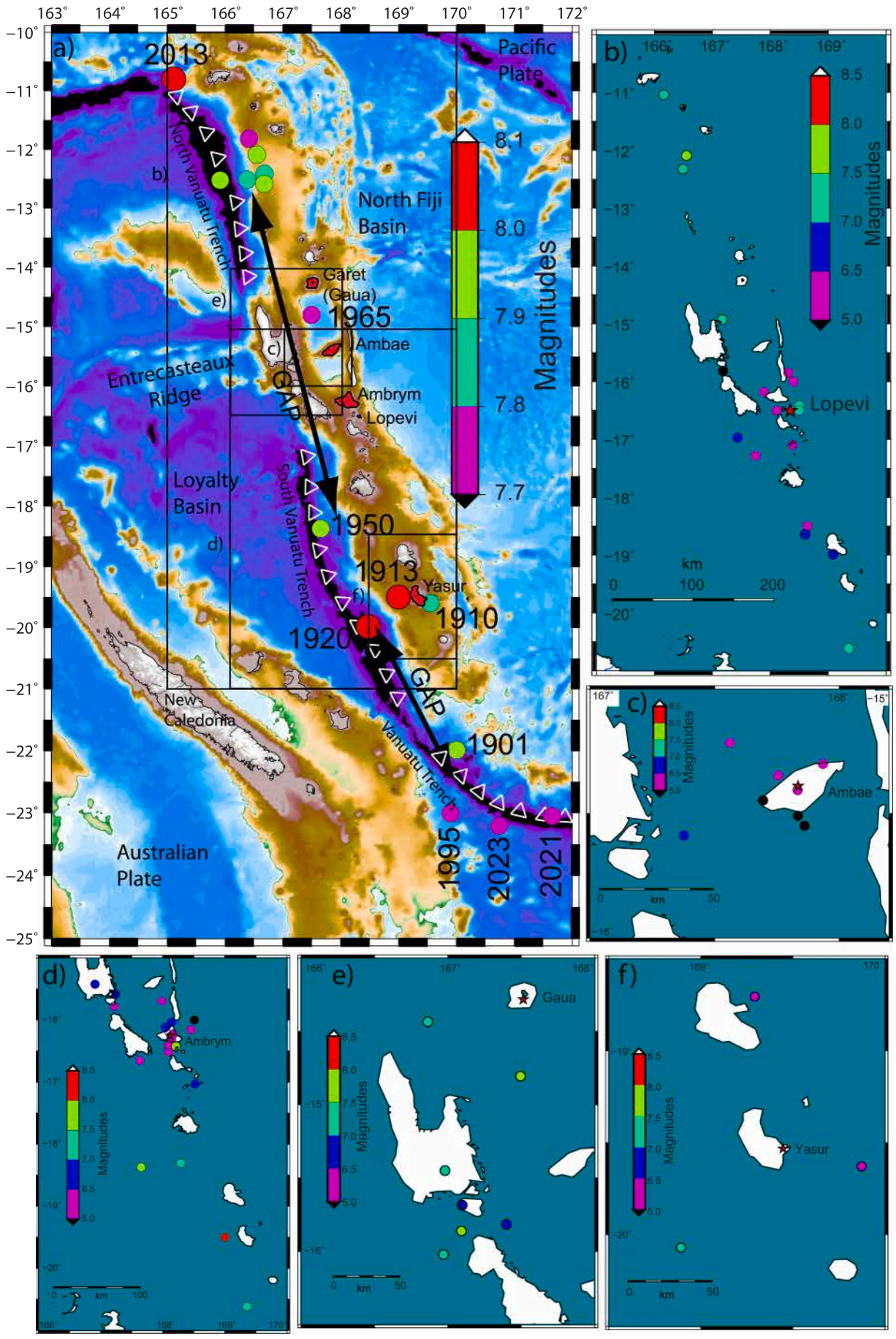

(caption on next page)

Fig. 1. a) Tectonic setting of the region. White triangles indicate the Vanuatu trench. Earthquakes plotted here (circles with color codes corresponding to magnitude) correspond to the ones quoted in the introduction. The two arrows represent potential seismic gaps. Islands with aerial active volcanoes are highlighted in red. Earthquakes that potentially triggered Lopevi (b), Ambae (c), Ambrym (d), Mount Garet (at Gaua) (e), and Yasur (f) volcanoes. (For interpretation of the references to color in this figure legend, the reader is referred to the web version of this article.)

Ngoru. Ambae island is located in front of the subduction-collision of the d'Entrecasteaux ridge (Daniel and Katz, 1981; Fig. 1). The magma composition at Ambae ranges from low-viscosity basalts to basaltic trachyandesites (Moussallam et al., 2019). Ambae has a relatively high-level SO_2 degassing. It ranked fifth in the list of large volcanic SO_2 degassing sources worldwide over the period of 2005–2015 (Carn et al., 2017). Bani et al. (2009a; 2012) have measured a high mean flux of 2.4 kt/d between 2004 and 2009. Despite this fact, its degassing trend shown by Moussallam et al. (2019) does not confirm a clear open-vent system. The conduit before the 2017–2018 eruption was mechanically closed with the magma within the plumbing system that was partially losing its magmatic gas at the surface. We consider Ambae as a closed-vent system according to the definition we used in this study. This is particularly true before the last 2017–2018 eruption, because 1) the magma is not always present at the surface and 2) the eruptive pattern consists into periods of eruptions separated by long quiescence periods. Ambae volcano has all the ingredients to host an active hydrothermal system because of the high level of rainfalls (~5 m /year), the presence of large water lakes at the summit of the volcano, and the presence of a rainforest (Bani et al., 2009a, 2009b). This hydrothermal system is well emphasized in the past phreatic eruptions, including the small (VEI = 2) phreatic eruption on 2 March 1995 (UTC, 3 March on LT) that sustained a vapor-and-ash column ~3 km high and a vapor plume that rose ~500 m on 4 March (UTC) (Robin et al., 1995; Rouland et al., 2001), and the Surtseyan eruptions that occurred in November–December 2005, followed by a rapid color change of the lake from light blue to red in May–June 2006 (Bani et al., 2009a; Németh and Cronin, 2009). The 2017–2018 sub-plinian eruption started on the 6 September 2017 with series of phreatic explosions, that opened a pathway for the magma to reach the surface on 22 September 2017. The event was followed by phreatic and phreatomagmatic manifestations, strombolian activity, and lava flows that ended in the end of 2018 (Moussallam et al., 2019; Park et al., 2021). Hence, the existence of an active hydrothermal system is well established on Ambae.

Ambrym island is a 35 km × 50 km volcano, with a summit elevation of ~1334 m above sea level. A 2 to 3 km wide rift crosses the island in a WNW-ESE direction, passing through the center of a large caldera. The magma composition at Ambrym ranges from low-viscosity basalts (McCall et al., 1970) to rare trachyandesites (Sheehan and Barclay, 2016). Ambrym mostly acts as an open-vent volcano, emitting persistent very-long-period tremors due to magma motions (Legrand et al., 2005). Since the mid-December 2018 eruption, Ambrym can be considered as a closed-vent system because no magma is directly in contact with the surface. Such change from open- to closed-event system is rare at Ambrym.

At an altitude of 800–900 m, the edifice is truncated by a 12 km-diameter summit caldera where two intra-caldera cones, Benbow (1160 m) and Marum (1270 m) frequently host several lava lakes (at least two within Benbow and several within Marum), whose number changed over time (McCall et al., 1970; Rouland et al., 2009; Bani et al., 2012; Allard et al., 2016; Moussallam et al., 2021). Marum and Benbow cones sustained a prodigious persistent degassing (mean SO_2 flux of ~5.4 kt/day, up to 33 kt/d between 2004 and 2009) directly from lava lakes. Short and vigorous periods of strombolian activity, mainly at Marum (Bani et al., 2009, 2012; Polacci et al., 2012; Allard et al., 2016; Coppola et al., 2016; Radebaugh et al., 2016), were superimposed at times to the typical activity, marked by a very close series of mild strombolian explosions. Ambrym was ranked as the largest volcanic SO_2 source worldwide based on the 2005–2015 period of Carn et al. (2017). This strong degassing had persisted over centuries and was firstly described by Captain James Cook in July 1774.

Mont Garet volcano on Gaua island is a 40 km wide stratovolcano truncated by a large summit caldera (6 km × 8 km) at 500–600 m above sea level, hosting the crater water lake Letas (Mallick and Ash, 1975; Bani et al., 2012, 2016). It presents a magmatic composition between basalt and trachyandesite (Métrich et al., 2016). There is a low but persistent degassing from Mt. Garet. The SO_2 flux was not measured recently but during the 2009–2010 eruption, up to >3 kt/d of SO_2 has been recorded (Bani et al., 2012). The degassing rose from a very low level of emission before the eruption (as expected in a closed-vent volcano). This volcano hosts an active hydrothermal system (Bani et al., 2012; Lages et al., 2020), as highlighted by the phreatic eruption of 1995 (Bani et al., 2012) and the phreatic to phreatomagmatic event that characterized the onset eruptive activity in 2009 (Bani et al., 2016). The summit caldera was also formed ~2000 years ago following a large hydromagmatic eruption (Robin et al., 1995). With our definition, Mont Garet is considered as a closed-vent volcano.

Lopevi is an iconic conical-shape 1413 m high volcano with historical activity occurring along a NW-SE fissure (rift zone) cutting across the volcano's summit. Its magma varies between high MgO basalts to low-magnesian basaltic andesites (Handley et al., 2008; Beaumais et al., 2013). Lopevi volcano produced the highest thermal anomalies detected over Vanuatu between 2000 and 2015 with weekly or monthly-long periods of activity interrupted by months or years of quiescent phases (Coppola et al., 2016). These clusters of thermal anomalies separated by quiescent periods that lasted months or years suggest that Lopevi behaves as a closed-vent volcano (Coppola et al., 2016). Lopevi volcanic degassing also observed discontinuity and between 2004 and 2009, the SO_2 emission rate was estimated between 0.156 kt/d to 0.98 kt/d (Bani et al., 2012). Such discontinuous and small degassing values are expected at a closed-vent volcano. An active hydrothermal system at Lopevi is yet to be confirmed, but it is strongly expected given the well-developed rift crossing the volcano and a high level of rainfalls in the region.

Yasur is a basaltic-trachyandesite to trachyandesite volcano located on the SE part of Tanna Island, with the Siwi caldera. It was formed following successive phases of active volcanism (Carney and McFarlane, 1979). The Siwi ignimbrites, 1–2 km^3 in magma volume and undated but probably <20 kyr ago, led to the formation of the Siwi caldera (Carney and McFarlane, 1979; Nairn et al., 1988; Robin et al., 1994; Allen, 2005; Métrich et al., 2011). The caldera (9 km × 4 km) hosts at its center part the Yenkahe resurgent dome (3 km × 5 km and 300 m high) with an axial graben, which may be associated to magmatic intrusions (Robin et al., 1994). Métrich et al. (2011) proposed that 25 km^3 of undegassed magma was accumulated beneath the Siwi caldera and was responsible of the rapid uplift of the Yenkahe bloc over the last 1000 years. Yasur volcano is located at the western end of Yenkahe dome. It is a small 361 m high pyroclastic cone and a typical open-vent volcano with a main crater of ~400 m in diameter divided into two sub-craters with at least three different vents (this number changes with time) where the tops of the magma columns are almost persistently exposed to the atmosphere. Yasur is a typical strombolian volcano, possibly for 630–850 years (Firth et al., 2014), with explosions occurring at a rate of one per 1–2 min (Spina et al., 2016; Woitischek et al., 2020). Gas volumes associated to large eruptions and a vigorous period of activity had been estimated for short periods at ~5000–80,000 m^3 from infrasonic studies (Iezzi et al., 2019), while it has been estimated at ~14,250 m^3 from open-path Fourier transform infrared spectroscopy combined with SO_2 flux measurements during a normal activity period (Woitischek et al., 2020). Yasur has a continuous degassing, with mean SO_2 emission

		Existence of an active hydro-thermal system	Number and list of eruptions triggered by earthquakes
Ambae 	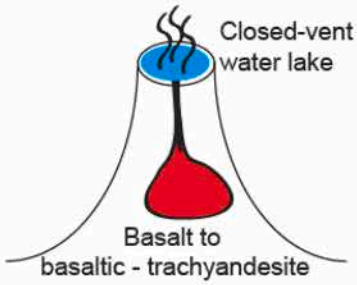	Yes	(3) 02/03/1995 (VEI=2) 27/11/2005 (VEI=2) 13/10/2017 (VEI=3)
Ambrym 	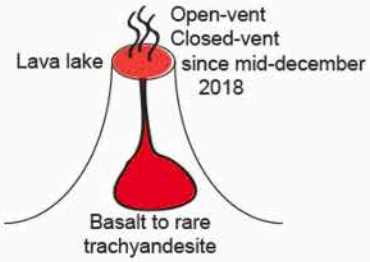	Possibly	(9) 14/19/1913 (VEI=3) 06/12/1950 (VEI=4) 15/08/1961 (VEI=3) 15/04/1972(VEI=3) 15/04/1973(VEI=3) 16/05/1980(VEI=3) 12/02/1988(VEI=3) 20/02/2015 (effusive) 15/12/2018 (effusive)
Garet (Gaua) 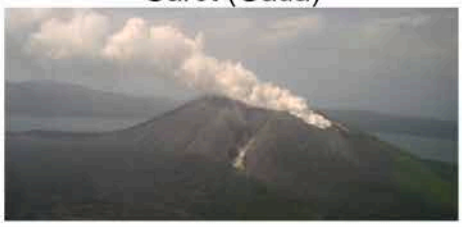	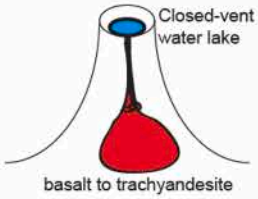	Yes	(2) 27/09/1965(VEI=3) 11/01/1974(VEI=2)
Lopevi 	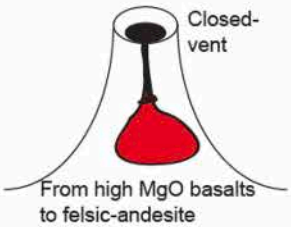	Possibly	(9) 01/11/1939(VEI=2) 10/07/1960(VEI=3) 07/07/1963(VEI=3) 27/01/1967(VEI=3) 15/04/1980(VEI=3) 16/07/1998(VEI=3) 08/06/2001(VEI=3) 08(06/2003(VEI=3) 21/04/2007(VEI=2)
Yasur (Tanna) 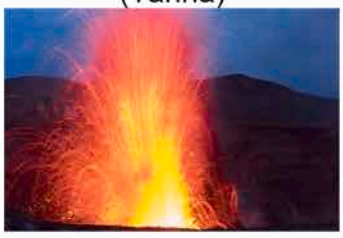	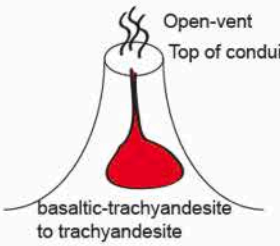	Yes	(0) No VEI No observed effusive activity

Fig. 2. List of the Vanuatu volcanoes with their main features (magma composition, closed/open vent volcano, presence of a lava or water lake, of a hydrothermal system, and the list of eruptions triggered by earthquakes). Ambae photo (25/09/2017): courtesy of T. Boyer. Marum (Ambrym, 16/09/2009): courtesy of M. Massat. Mont Garet (25/01/2007) courtesy of P. Bani. Lopevi (11/03/2008) courtesy of Mr. Marini. Yasur (19/08/2016) courtesy of T. Boyer.

rate of ~630–680 t.d^{-1} (from <200 to 1.5 kt/d) measured between 2004 and 2009 and a relatively high heat flow of ~10^9W (Bani and Lardy, 2007; Métrich et al., 2011; Bani et al., 2012), as expected for an open-vent volcano. The volcano is known for its frequent strombolian explosions (a few tens per hour), several vulcanian eruptions and rare lava flows (Carney and McFarlane, 1979). It was ranked eleventh in the list of SO_2 emitters worldwide in the 2005–2015 period (Carn et al., 2017). Thermal activity recorded on satellites was almost continuous between 2000 and 2015 (Coppola et al., 2016), confirming its open-vent character. The present and continuous strombolian activity seems similar to the one described by Captain James Cook in 1774 when he arrived on Tanna Island onboard the sloop HMS "Resolution" belonging to the Royal Navy. A shallow and very active hydrothermal system is present throughout the caldera around Yasur volcano, with most active parts associated with the Yenkahe dome, as shown from geophysical measurements (Brothelande et al., 2016). The hydrothermal areas are mainly mapped by the unvegetated and altered surface induced by high thermal flux across the areas of Yenkahe dome, but most specifically by its eastern side where the presence of many faults can be observed as well as some extended altered surface of the dome. The outer caldera ring fault is also bordered by a hydrothermal area, suggesting that it is an efficient guide for the flow of hydrothermal fluids (Brothelande et al., 2016).

4. Method

To determine which earthquakes could modify the volcanic behavior of Vanuatu's volcanoes, we applied a three-step procedure:

1) We listed all published cases where an earthquake has been suggested as potentially triggering source for volcanic unrest or eruption across the Vanuatu arc.
2) We calculated the TRIGI index for all these cases to confirm that most of them correspond to near-field earthquake-volcano distances.
3) We looked at the most significant eruptions (VEI $\geq$ 3 of the Smithsonian catalogue: https://volcano.si.edu) not necessarily mentioned in the literature and examined the earthquakes (in the USGS catalogue) that occurred in the six-month period preceding the eruption with the smallest index value.

In step 1), the largest explosions are generally described based on their VEI (Table 1) whilst small volcanic manifestation corresponds to effusive lava-flow without associated explosion (thus without VEI). The description of the volcanic activity is provided in Table 1. For example, the 2015 and 2018 effusive eruptions on Ambrym volcano are well present in the literature but are not quantified with a VEI (see references in Table 1). The Yasur volcano, which has almost constant strombolian activity, has no corresponding reported VEI. Sometimes, the description in the literature corresponds to the variations of geophysical and geochemical parameters such as seismic, acoustic, thermal, lava lake level, and gas emission and composition data, as summarized in Table 1. They correspond to relative changes in volcanic activity evolving towards low-level magmatic processes and non-explosive events.

For each case, we calculated the following parameters (given in Table 1):

1) the length (L) and width (W) of the earthquake rupture surface S = LW. They are calculated from the magnitude M depending on the focal mechanism (reverse, normal and strike-slip) using the following scaling-law relations of Blaser et al. (2010):

$$\text{Reverse fault}: L = 10^{(-2.28+0.55\,M)}\ W = 10^{(-1.8+0.45\,M)}$$

$$\text{Normal fault}: L = 10^{(-1.61+0.46\,M)}\ W = 10^{(-1.08+0.34\,M)}$$

$$\text{Strike-slip fault}: L = 10^{(-2.56+0.62\,M)}\ W = 10^{(-0.66+0.27\,M)}$$

2) the earthquake-volcano epicentral distance d; the triggering index TRIGI = $d/\sqrt{S}$ which is the ratio of this distance (d) with respect to the characteristic length of the earthquake ($\sqrt{S}$: square root of the rupture surface);
3) the time-delay between the earthquake and the related enhanced volcanic activity.

5. Data and results

5.1. Cases found in the literature for Vanuatu volcanoes

In the existing literature, we identified 30 cases of volcanic activity documented in Vanuatu, which may have been triggered by earthquakes (Table 1).

They correspond to relatively large explosions (VEI $\geq$ 2) on Vanuatu volcanoes that were preceded by a potentially triggering earthquake. For example, Linde and Sacks (1998) proposed a causal link between the 14 October 1913 (M8.1) earthquake and the VEI = 3 Ambrym eruption that occurred on the same day, as well as the 10 January 1974 (M7.2) earthquake that occurred one day before the VEI = 2 eruption of Gaua. Another case is the 2 December 1950 (M7.9) earthquake that occurred four days before the large VEI = 4 eruption of Ambrym (Brodsky et al., 1998; Manga and Brodsky, 2006). On Lopevi volcano, Priam (1964) mentioned three earthquakes that preceded (between 74 and 81 days) the November 1939 (VEI = 2) eruption, two earthquakes before (124 and 103 days) the July 1960 (VEI = 3) eruption, one earthquake before (120 days) the lava flow in July 1962, and one earthquake occurring before (119 days) the July 1963 (VEI = 3) eruption (Table 1). Blot (1981) suggested that several deep earthquakes (100–300 km depth) beneath the Ambrym, Epi, Karua, and Lopevi volcanoes were related to their activities due to their spatio-temporal correlations. However, we have only considered here the three largest eruptions for which we were able to find the location and magnitude of the earthquake in the USGS catalogue and a VEI associated with the volcano in the Smithsonian webpage (Table 1). For this reason, the 1901 and 1970 Karua eruptions mentioned by Blot (1981) are not considered here because their existence are questioned by the Smithsonian webpage. Avouris et al. (2017) mentioned a M7.2 earthquake that occurred 27 days before the Lopevi eruption of 21 April 2007 (VEI = 2). Other cases found in the literature are given in Table 1.

Other cases found in the literature corresponds to subtle changes in volcanic activity, hence without an eruptive event (Table 1). As explained above, these subtle volcanic changes are not characterized by a VEI. We thus rely on the literature to find information on changes of volcanic activity after a large earthquake (Table 1). The 2015 and 2018 effusive flows on Ambrym volcano are good examples where the VEI was not determined to classify the events although significant geophysical changes were recorded after the large earthquakes preceding these two eruptions. The 20 February 2015 intra-caldera effusive eruption occurred 30 h after the 19 February M6.4 earthquake which was located at 20 km away (Hamling and Kilgour, 2020; Firth and Cronin, 2023; Shreve et al., 2021). The heat flux significantly increased before the intra-caldera effusive eruption of 20 February 2015 (Firth and Cronin, 2023). Such increase is linked to the rising level of the magma, a process that heralds an eruption. The 19 February 2015 earthquake may have significantly contributed to the 20 February eruption. The very large effusive eruption of 15 December 2018 was preceded on the same day by an M5.4 earthquake located 21 km away (Shreve et al., 2019; Moussallam et al., 2021) in addition to an M6.5 earthquake located 24 km away (Firth and Cronin, 2023) that occurred 116 days before. Other cases taken from the literature are given in Table 1. The histogram of the TRIGI indexes corresponding to these cases identified in the literature is displayed in yellow in figure2. Hence, most (21) of the 30 triggering

Table 1
List of the triggering earthquakes with their date, hour, magnitude, focal mechanism when available, length (L) and width (W) of the rupture surface, location (latitude, longitude). For the oldest earthquakes (from 1913 to 1987), the focal mechanism is generally unknown. As they are located near the trench, we supposed that they are reverse faults. List of the volcanoes which activity is related to the earthquake with their name, location (latitude, longitude), date of eruption when available, the earthquake-volcano epicentral distances (d), the TRIGI indexes $d/\sqrt{S}$ where S = LW, and the time-delay between the earthquake and the volcanic activity. Description of the volcanic activity, with the VEI when available.

Earthquakes							volcanoes				Eq/volcano			e		
Date	Hour	Mag	L (km)	W (km)	Latitude	Longitude	Name	Latitude	Longitude	Date eruption	Distance (km)	$d/\sqrt{S}$	Time delay (days)	J/m3	Description of the kind of volcanic changes	References
14-10-1913	08:08	8.1	150	70	−19.5	169	Ambrym	−16.25	168.12	14-10-1913	373	3.6	0	0.213	VEI = 3 Major flank phreato-magmatic eruption Large eruption on 5 and 6 December 1913 Partial evacuation in 1913–15	Linde and Sacks (1998) (VEI from Smithsonian) Manga and Brodsky (2006)
12-08-1939		7.2	48	28	−16.417	168.5	Lopevi	−16.51	168.346	01-11-1939	19	0.5	81	81.61	Birth of a new crater in the NW flank. VEI = 2	Priam (1964)
18-08-1939	22:16	6.5	20	13	−18.643	168.603	Lopevi	−16.51	168.346	01-11-1939	239	14.7	75	0.004	Birth of a new crater in the NW flank. VEI = 2	Priam (1964)
19-08-1939	00:47	6.1	12	9	−18.498	168.641	Lopevi	−16.51	168.346	01-11-1939	224	21.9	74	0.001	Birth of a new crater in the NW flank. VEI = 2	Priam (1964)
06-12-1948	12:10	6.1	12	9	−17.408	168.099	Karua	−16.83	168.536	01-04-1949	79	7.7	116	0.03	VEI = 3	This study. Day unknown, we put it as first of the month
21-07-1950	20:32	6.4	17	12	−16.156	168.457	Ambrym	−16.25	168.12	06-12-1950	37	2.6	138	0.779	VEI = 4 Activity continues until 25 November 1951	This study
02-12-1950	19:51	7.9	116	57	−18.373	167.654	Ambrym	−16.25	168.12	06-12-1950	241	3	4	0.407	VEI = 4 Activity continues until 25 November 1951	Brodsky et al. (1998); Manga and Brodsky (2006) Mag USGS
18-10-1952	05:22	6.3	15	11	−15.868	167.675	Epi	−16.68	168.36	12-02-1953	116	9	117	0.018	Submarine eruption from 3 craters simultaneously. A cone was formed above sea level, rapidly demolished VEI = 3 (Smithsonian)	Blot (1981)
03-07-1959	17:55	6.6	22	15	−16.275	173.065	Karua	−16.83	168.536	18-09-1959	487	26.8	77	7E-04	Large phreatic eruption	Blot (1981)
08-03-1960		7.1	42	25	−16.5	168.5	Lopevi	−16.51	168.346	10-07-1960	16	0.5	124	98.09	Plinian eruption (nuée ardente) with permanent evacuation of people. Birth of a new crater in the NW flank. VEI = 3	Priam (1964)
29-03-1960	06:31	6.7	25	16	−16.97	167.433	Lopevi	−16.51	168.346	10-07-1960	110	5.4	103	0.08	Plinian eruption (nuée ardente) with permanent evacuation of people. Birth of a new crater in the NW flank. VEI = 3	Priam (1964) Blot (1981)
23-07-1961	21:51	7.3	56	32	−18.307	168.29	Ambrym	−16.25	168.12	15-08-1961	229	5.4	23	0.072	VEI = 3 Strong activity on 9 January 1962 and 7 November 1962	This study
18-03-1962	03:06	6	10	8	−16.507	168.108	Lopevi	−16.51	168.346	16-07-1962	25	2.7	120	0.67	Lava flow	Priam (1964)
10-03-1963		6	10	8	−16	168.4	Lopevi	−16.51	168.346	07-07-1963	57	6.2	119	0.057	VEI = 3 The most recent parasitic crater formed in 1963 at the NW part of the summit along the NW-SE fissure system	Priam (1964) Warden (1967)

(*continued on next page*)

Table 1 (*continued*)

Earthquakes							volcanoes				Eq/volcano			e		
Date	Hour	Mag	L (km)	W (km)	Latitude	Longitude	Name	Latitude	Longitude	Date eruption	Distance (km)	d/$\sqrt{S}$	Time delay (days)	J/m3	Description of the kind of volcanic changes	References
01-05-1963	10:03	6.8	29	18	−18.984	169.084	Lopevi	−16.51	168.346	07-07-1963	286	12.5	67	0.006	VEI = 3 Same description as before	This study.
20-05-1965	00:40	7.7	90	46	−14.805	167.495	Garet	−14.28	167.514	27-09-1965	58	0.9	130	15.06	VEI = 3	This study
11-08-1965	03:40	7.2	48	28	−15.449	166.98	Garet	−14.28	167.514	27-09-1965	142	3.9	47	0.195	VEI = 3	This study
11-08-1965	19:52	6.9	33	20	−15.685	167.097	Garet	−14.28	167.514	27-09-1965	162	6.3	47	0.049	VEI = 3	This study
11-08-1965	22:31	7.6	79	42	−15.861	167.092	Garet	−14.28	167.514	27-09-1965	181	3.1	47	0.356	VEI = 3	This study
12-08-1965	08:01	6.9	33	20	−15.817	167.399	Garet	−14.28	167.514	27-09-1965	171	6.7	46	0.041	VEI = 3	This study
13-08-1965	12:40	7.4	62	34	−16.022	166.97	Garet	−14.28	167.514	27-09-1965	202	4.4	45	0.132	VEI = 3	This study
31-12-1966	18:23	7.8	102	51	−12.091	166.552	Lopevi	−16.51	168.346	27-01-1967	528	7.3	27	0.028	VEI = 3	This study
31-12-1966	22:15	7.1	42	25	−12.326	166.491	Lopevi	−16.51	168.346	27-01-1967	506	15.6	27	0.003	VEI = 3 Strong activity on 1 March 1967	This study
27-10-1971	17:58	6.8	29	18	−15.582	167.246	Ambrym	−16.25	168.12	15-04-1972	119	5.2	171	0.088	VEI = 3 Activity 28 July 1972 and	This study
06-03-1972	02:42	5.9	9	7	−16.654	167.629	Ambrym	−16.25	168.12	15-04-1972	69	8.5	40	0.023	VEI = 3 Activity 28 July 1972 and	This study
06-03-1972	02:42	5.9	9	7	−16.654	167.629	Ambrym	−16.25	168.12	15-04-1972	69	8.5	40	0.023	VEI = 3	This study
08-04-1973	12:41	6.4	17	12	−15.779	167.218	Ambrym	−16.25	168.12	15-04-1973	110	7.6	7	0.03	VEI = 3 Activity on December 1973; 20 December 1974; 24 May 1976	This study
10-01-1974	08:51	7.2	48	28	−14.434	166.863	Garet	−14.28	167.514	11-01-1974	72	2	1	1.5	VEI = 2	Linde and Sacks (1998)
08-12-1979	08:31	5.6	6	5	−15.845	168.311	Lopevi	−16.51	168.346	15-04-1980	74	12.9	129	0.007	VEI = 3	This study
08-12-1979	08:31	5.6	6	5	−15.845	168.311	Ambrym	−16.25	168.12	16-05-1980	49	8.5	160	0.024	VEI = 3 Activity on 23 July 1980	This study
02-10-1987	10:06	5.1	3	3	−16.326	168.131	Ambrym	−16.25	168.12	12-02-1988	9	2.8	133	0.727	VEI = 3 intense swarm of earthquakes before eruption Activity continues with VEI = 2 on 24/04/1989 and VEI = 2 on 16/09/1990	This study
26-11-1987	13:33	6.2	19	8	−16.373	168.117	Ambrym	−16.25	168.12	12-02-1988	14	1.1	78	7.407	VEI = 3 Same description as before	This study
27-11-1987	13:05	5.5	6	5	−16.263	168.132	Ambrym	−16.25	168.12	12-02-1988	2	0.4	77	249.4	VEI = 3 Same description as before	This study
27-11-1987	13:11	5.5	6	5	−16.307	168.141	Ambrym	−16.25	168.12	12-02-1988	7	1.4	77	5.817	VEI = 3 Same description as before	This study
27-11-1987	13:33	6.2	19	8	−16.373	168.117	Ambrym	−16.25	168.12	12-02-1988	14	1.1	77	7.407	VEI = 3 Same description as before	This study
27-11-1987	17:35	5.1	3	3	−16.224	168.166	Ambrym	−16.25	168.12	12-02-1988	6	1.9	77	2.452	VEI = 3 Same description as before	This study
04-12-1994	19:02	5.4	5	4	−15.347	167.754	Ambae	−15.39	167.835	02-03-1995	10	2.2	88	1.432	VEI = 2 Phreatic eruption on 02/03/1995 (3 March in LT) with increased gas emissions and seismicity, with a vapor-and-ash column ~3 km high. A vapor plume rose ~500 m on 4 March (UTC).	Wiart (1995) Robin et al. (1995) Rouland et al. (2001)
05-12-1994	00:46	5.1	3	3	−15.3	167.935	Ambae	−15.39	167.835	02-03-1995	15	4.6	87	0.157	VEI = 2 Same description as before	Robin et al. (1995) Rouland et al. (2001)
05-12-1994	15:50	5.1	3	3	−15.405	167.833	Ambae	−15.39	167.835	02-03-1995	2	0.6	87	66.21	VEI = 2 Same description as before	Robin et al. (1995) Rouland et al. (2001)
16-07-1998	11:56	7	37	22	−11.04	166.16	Lopevi	−16.51	168.346	16-07-1998	652	22.6	0	0.001	VEI = 3	This study. Many triggered earthquakes

(*continued on next page*)

Table 1 (*continued*)

Earthquakes							volcanoes				Eq/volcano			e		
Date	Hour	Mag	L (km)	W (km)	Latitude	Longitude	Name	Latitude	Longitude	Date eruption	Distance (km)	d/$\sqrt{S}$	Time delay (days)	J/m3	Description of the kind of volcanic changes	References
																towards the south (towards Lopevi)
22-08-1999	12:40	6.6	22	15	−16.117	168.039	Ambrym	−16.25	168.12	23-08-1999	17	0.9	1	15.58	Earthquake very strongly felt by people (MM Intensity of VI on the volcano). One day after the earthquake, a new vent had opened on the Benbow crater floor that was continually emitting light brown ash that rose 1500 m above the crater floor (~2300 m altitude) before being blown to the S. From 16:15 to 16:25 on 27 August there were 66 discrete explosions or loud venting noises heard from the crater. At one location on the NW rim of the central crater, 200 m from the new vent, a recent ash deposit was ~50 m thick.	Volcanism Program, 1999. Report on Ambrym (Vanuatu) (Wunderman, R., ed.). *Bulletin of the Global Volcanism Network*, 24:8. Smithsonian Institution. https://doi.org/10.5479/si.GVP.BGVN199908-257040
26-11-1999	13:21	7.5	70	38	−16.423	168.214	Ambrym	−16.25	168.12	19–01–2000	22	0.4	54	142.1	MODIS detected quasi-continuous thermal alerts for Ambrym throughout 2001 and 2002. Anomalies continued in January–February 2003.	Carniel et al. (2003) Global Volcanism Program https://volcano.si.edu/showreport.cfm?doi=10.5479/si.GVP.BGVN200301-257040 Firth and Cronin (2023)
09-08-2000	00:08	6.3	15	11	−15.693	167.986	Ambrym	−16.25	168.12	09-08-2000	64	5	0	0.108	Increase of amplitudes of two seismic frequencies staring the same day and during one more day, and increase of the tremor number a few days after the Eq	Carniel et al. (2003) Rouland et al. (2009)
09-08-2000	17:02	4.4	1	2	−16	168.51	Ambrym	−16.25	168.12	09-08-2000	50	34.6	0	4E-04	Increase of amplitudes of two seismic frequencies staring the same day and during one more day, and increase of the tremor number a few days after the Eq	Carniel et al. (2003)
04-10-2000	16:58	6.8	29	18	−15.421	166.91	Ambrym	−16.25	168.12	07-10-2000	159	6.9	3–4	0.037	Increase of the tremor number a few days after the Eq and lasting a few days	Rouland et al. (2009)
09–01–2001	16:49	7.1	42	25	−14.928	167.17	Lopevi	−16.51	168.346	08-06-2001	216	6.7	150	0.04	VEI = 3	This study
14-04-2001	08:51	5.6	8	6	−17.093	168.383	Lopevi	−16.51	168.346	08-06-2001	65	9.5	55	0.01	VEI = 3	This study
07-10-2002	19:00	5.6	6	5	−18.706	169.293	Yasur	−19.53	169.447	08-10-2002	93	16.2	1.1	0.003	Thermal anomaly	Delle Donne et al. (2010)
05-04-2003	22:03	5.9	9	7	−16.18	167.889	Lopevi	−16.51	168.346	08-06-2003	61	7.5	64	0.033	VEI = 3	This study
13-05-2003	21:21	6.3	15	11	−17.287	167.744	Lopevi	−16.51	168.346	08-06-2003	108	8.4	26	0.022	VEI = 3	This study
03-10-2004	18:38	5.1	5	5	−19.629	169.874	Yasur	−19.53	169.447	06-10-2004	46	9.3	2.8	0.005	Thermal anomaly	Delle Donne et al. (2010)

(*continued on next page*)

Table 1 (*continued*)

Earthquakes							volcanoes				Eq/volcano			e		
Date	Hour	Mag	L (km)	W (km)	Latitude	Longitude	Name	Latitude	Longitude	Date eruption	Distance (km)	d/$\sqrt{S}$	Time delay (days)	J/m3	Description of the kind of volcanic changes	References
23-07-2005	01:04	5.5	6	5	−15.216	167.561	Ambae	−15.39	167.835	27–11–2005	35	6.8	127	0.047	VEI = 2 surtseyan eruption	This study. Similar earthquake as the one before
13–11–2005	05:42	4.8	2	2	−15.818	167.185	Lopevi	−16.51	168.346	19–11–2005	146	63.7	6	6E-05	Thermal anomaly	Delle Donne et al. (2010)
25-03-2007	00:40	7.1	42	25	−20.617	169.357	Ambrym	−16.25	168.12		503	15.5		0.003	changes in SO2 rate	Avouris et al. (2017)
25-03-2007	00:40	7.1	42	25	−20.617	169.357	Lopevi	−16.51	168.346	21-04-2007	469	14.5	27	0.004	VEI = 2	Avouris et al. (2017)
01-04-2007	20:39	8.1	150	70	−8.466	157.043	Ambrym	−16.25	168.12		1481	14.5		0.003	changes in SO2 rate	Avouris et al. (2017)
01-04-2007	20:39	8.1	150	70	−8.466	157.043	Lopevi	−16.51	168.346	21-04-2007	1517	14.8	20	0.003	VEI = 2	This study by suggestion of Avouris et al. (2017)
09-04-2008	12:46	7.3	54	31	−20.071	168.892	Yasur	−19.53	169.447	09-04-2008	83	2	0	1.364	Change (complete disappearance or appearance) of earthquake families (of similar waveforms) after the Eq. Drop of the rate of LP events (related to deep process) after the Eq. Change of medium velocity commitment to the earthquake, by using coda wave interferometry	Battaglia et al. (2012) Battaglia et al. (2016b) Battaglia et al. (2016a)
23–01–2015	03:47	6.8	29	18	−17.031	168.52	Ambrym	−16.25	168.12	20-02-2015	97	4.2	28	0.163	See the description of the volcanic activity in the 19/02/2015 (13:18) earthquake	This study suggested by a similar earthquake of the the study of Shreve et al. (2021) and Firth and Cronin (2023)
19-02-2015	13:18	6.4	17	12	−16.431	168.148	Ambrym	−16.25	168.12	20-02-2015	20	1.4	1	4.931	Intra-caldera effusive eruption the 20/02/2015 (21 at LT), 30 h after the earthquake. Creation of a new vent within the main summit caldera floor (reactivated in 2018) with a minor flank lava flow. Decrease of heat flux >200 MW immediately following the 2015 eruption and earthquake due to the fall of the level of the two lava lakes (Coppola et al., 2016; Wright 2016)	Hamling and Kilgour (2020) Shreve et al. (2021) Firth and Cronin (2023)
19-02-2015	13:23	5.2	4	3	−16.454	168.109	Ambrym	−16.25	168.12	20-02-2015	23	6.3	1	0.061	See the description of the volcanic activity in the 19/02/2015 (13:18) earthquake	This study suggested by a similar earthquake of the the study of Shreve et al. (2021) and Firth and Cronin (2023)
19-02-2015	14:32	5.4	5	4	−16.513	168.091	Ambrym	−16.25	168.12	20-02-2015	29	6.3	1	0.059	See the description of the volcanic activity in the 19/02/2015 (13:18) earthquake	This study suggested by a similar earthquake of the the study of Shreve et al. (2021) and Firth and Cronin (2023)
19-02-2015	19:56	5.1	3	3	−16.394	168.095	Ambrym	−16.25	168.12	20-02-2015	16	4.9	1	0.129	See the description of the volcanic activity in the 19/02/2015 (13:18) earthquake	This study suggested by a similar earthquake of the the study of Shreve et al. (2021) and Firth and Cronin (2023)

(*continued on next page*)

Table 1 (*continued*)

Earthquakes							volcanoes				Eq/volcano			e		
Date	Hour	Mag	L (km)	W (km)	Latitude	Longitude	Name	Latitude	Longitude	Date eruption	Distance (km)	d/$\sqrt{S}$	Time delay (days)	J/m3	Description of the kind of volcanic changes	References
01-04-2017	04:01	4.8	2	2	−15.447	167.694	Ambae	−15.39	167.835	13-10-2017	16	7	195	0.048	VEI = 3	This study
07-04-2017	16:29	4.5	2	2	−15.509	167.834	Ambae	−15.39	167.835	13-10-2017	13	8	189	0.033	VEI = 3	This study
09-05-2017	13:52	6.8	29	18	−15.588	167.377	Ambae	−15.39	167.835	13-10-2017	54	2.4	157	0.944	VEI = 3	This study
29-06-2017	20:39	4.6	2	2	−15.549	167.861	Ambae	−15.39	167.835	13-10-2017	18	9.9	106	0.017	VEI = 3	This study
21-08-2018	22:32	6.5	20	13	−16.032	168.143	Ambrym	−16.25	168.12	15-12-2018	24	1.5	116	3.975	Intra-caldera effusive eruption the 15/12/2018 Drainage of Benbow and Marum lava lakes the 17 December 2018. Heat flux decreases of ~33 MW at Marum lava lake	Firth and Cronin (2023)
15-12-2018	20:22	5.4	6	5	−16.416	168.22	Ambrym	−16.25	168.12	15-12-2018	21	3.8	0	0.155	Very large eruption. Within 12 h after the beginning of the eruption, drop in lava lake level and followed on 17 December by magma propagation into the SE rift zone and reached the sea. A visual observation on 16 December confirms that all the 5 lava lakes were drained. Intra- and extra-caldera eruption. Changes in thermal index, VT seismic rate, deformation, SO_2 flux. Very large persistent degassing. SO2 degassing mainly took place on 15 and 16 December, ceasing early in the morning of 16 December (UT) Magma mixing between 15 and 17 December and dyke propagation. Submarine eruption just off the SE coast of the island. Uplift of the eastern rift and subsidence of the caldera floor during the eruption. Petrological studies strongly suggest a rapid magma mixing which coincide with the occurrence of the earthquake (Moussallam et al., 2021).	Shreve et al. (2019) Moussallam et al. (2021)

indexes are ≤10, corresponding to 70% of the cases found in the literature. These small indexes (≤10) reveal that the earthquake-volcano distances are within the near-field.

5.2. New cases proposed for Vanuatu volcanoes

In the literature, not all the largest eruptions (VEI ≥ 3) have been linked to a potentially triggering earthquake for Vanuatu volcanoes. We therefore attempt to complete this list. We considered the 12 additional eruptions (VEI ≥ 3) reported by the Smithsonian website on all volcanoes in Vanuatu and searched among all the earthquakes worldwide the associated potentially triggering earthquake that occurred up to six months before the eruption with the smallest TRIGI value (Table 1). They correspond to five eruptions at Ambrym (in 1950; 1961; 1972; 1980; 1988), five eruptions at Lopevi (in 1963; 1980; 1998; 2001; 2003), one eruption at Garet in 1965; and one eruption at Ambae in 2017 (Table 1). All these eruptions were associated with a triggering earthquake. For example, we found a particular tectonic-earthquake swarm that occurred in 1965 in the near-field of Garet volcano, with the following characteristics: it was composed of six earthquakes of magnitudes between 6.9 and 7.7, five of which occurred within <3 days. This swarm occurred one and half month before the large (VEI = 3) eruption at Garet volcano. Another example relates to the M6.4 earthquake of 19 February 2015, located at 20 km distance from Ambrym volcano, that was linked to the small effusive phase of 20 February 2015 (21 at LT), occurring thirty hours after the earthquake (Hamling and Kilgour, 2020; Shreve et al., 2021; Firth and Cronin, 2023). We added to this earthquake three additional earthquakes of magnitude from 5.1 to 5.4 that occurred on the same day (19 February 2015 UTC) at short distances (from 16 to 29 km), with a small TRIGI ranging from 4.9 to 6.3. Additionally, a fifth M6.8 earthquake occurred on 23 January 2015, 28 days before the eruption, also with a small TRIGI of 4.2. These four new near-field earthquakes, may have potentially clock-advanced the 2015 effusive eruption in the same way as the M6.4 earthquake mentioned by Hamling and Kilgour (2020); Shreve et al. (2021); and Firth and Cronin (2023). The new set of 39 cases are listed in Table 1 and referenced as "This study". They are shown in red in Fig. 3 and show similar characteristics to those found in the literature, with most (34) of the 39 cases (87%) corresponding to near-field earthquake-volcano distances (indexes ≤10).

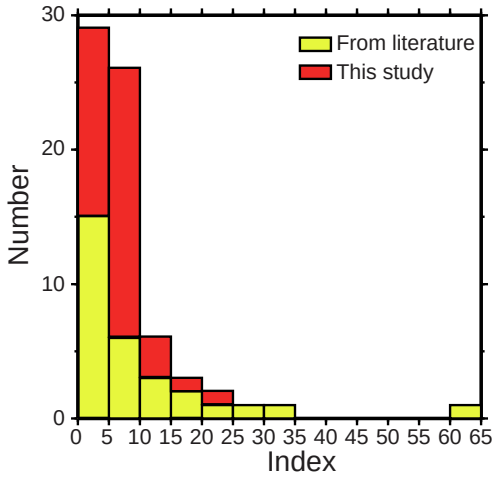

Fig. 3. Histogram of TRIGI indexes corresponding to Vanuatu volcanoes (Table 1). Small indexes (≤10) correspond to near-field earthquake-volcano distances, and indexes larger than 10 correspond to far-field earthquakes. Yellow histogram corresponds to the 30 cases found in the literature; red histogram corresponds to the new 39 cases of this study. (For interpretation of the references to color in this figure legend, the reader is referred to the web version of this article.)

5.3. Time-delay between the potentially triggering earthquake and volcanic activity

A histogram of the time-delay (Table 1) between the occurrence of the potentially triggering earthquake and the associated volcanic activity is displayed in Fig. 4, with a bin of one day. The maximum time delay is ~200 days and 16 (24%) occurring within a week after the occurrence of the potentially triggering earthquake and 47 (68%) within 3 months.

5.4. Distance versus magnitude relationship

Many past works (e.g., Manga, 2001; Manga and Brodsky, 2006; Wang et al., 2006; Manga and Wang, 2007; Wang, 2007) have studied the liquefaction effects, the mud volcanoes and streamflows following earthquakes by looking at the distance versus the earthquake magnitude. Similarly, we plot the earthquake-volcano distances versus magnitude in a $\log_{10}$-linear plot for the Vanuatu volcanoes according to Table 1 (Fig. 5). The colors indicate the main volcanoes. We group two volcanoes (Karua and Epi) in a single color because we have only three cases for them. Circles correspond to the near-field (TRIGI≤10) distances, squares to the far-field (TRIGI>10) distances. We added in Fig. 5 (black lines) the theoretical maximum distances "d_{max}" below which an earthquake (of a given magnitude) can trigger a volcanic activity in the near-field (corresponding to a TRIGI index of 10, thus $d_{max} = 10.\sqrt{S}$ and a TRIGI index of 1), for the three main focal mechanism types (reverse, normal and strike-slip). This maximum distance is estimated for each magnitude by calculating first the length (L), the width (W), and the surface S = LW of the rupture plane depending on the focal mechanism using the scaling laws of Blaser et al. (2010). The three curves corresponding to reverse, normal, and strike-slip focal mechanism types are very close (Fig. 5), showing that focal mechanism type is not the main feature responsible of the potential reactivation of a volcanic activity. The nondimensional index is instead of first order importance (see the difference in Fig. 5 for indexes of 1 and 10).

Note that earthquakes of intermediate magnitudes, for example around M5 or M6, can trigger a volcanic activity at shorter distances than for a large earthquake (M7+). For example, on Ambrym volcano, eight earthquakes of magnitude between 5 and 5.5 (Table 1) were located at distances between 2 km and 29 km from the volcano (Fig. 1d).

Three cases of earthquakes that possibly triggered volcanic activity are clearly located in far-field distances (corresponding to the largest indexes in Table 1 and indicated in Fig. 5). One of them is the 3 July 1959 M6.6 earthquake, located 487 km from Karua volcano, which led

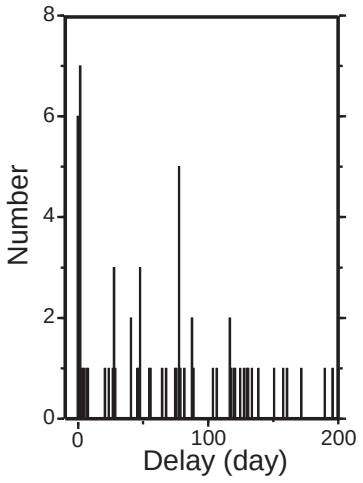

Fig. 4. Time-delay between the potentially triggering earthquake and volcanic eruption or unrest at Vanuatu volcanoes (Table 1). Bin of one day. This figure repeats an analysis first done by Linde and Sacks (1998).

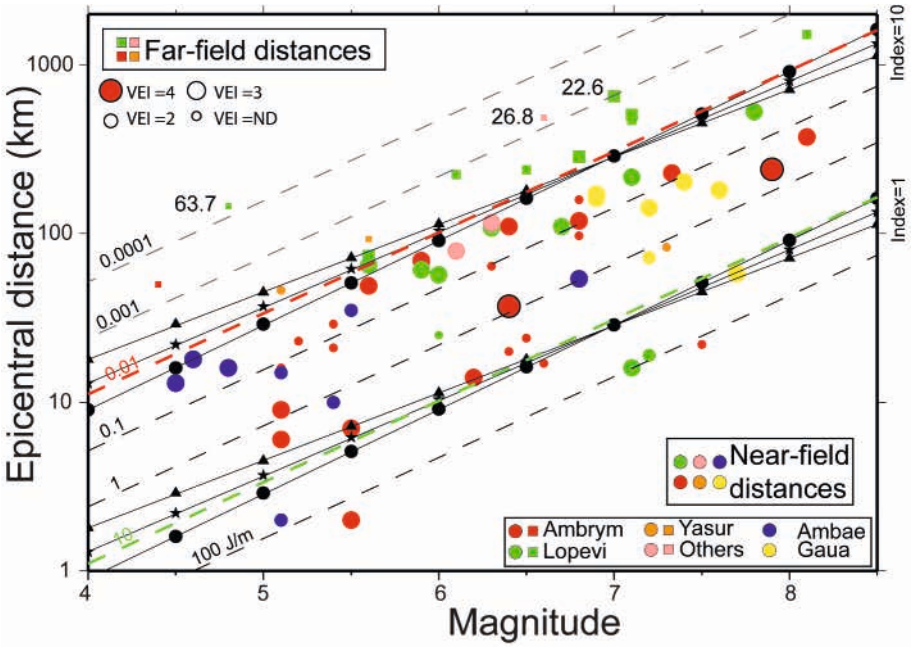

Fig. 5. Distribution of the volcanic activity changes plotted in a $\log_{10}$-linear axis of the epicentral distance versus magnitude M corresponding to the Vanuatu volcanoes of Table 1. The different colors correspond to the different volcanoes. "Others" correspond to the Karua and Epi volcanoes. Colored dots correspond to near-field earthquake-volcano distances (index ≤10) and colored squares to far-field distances (index>10). We added the theoretical maximum distance curves (black lines) for each magnitude corresponding to normal (triangle), reverse (circle) and strike-slip (asterisk) focal mechanism, for an index of 10 and an index of 1. The size of the symbols defines the VEI. The smaller size corresponds to volcanic changes that are not explosions and for which the VEI are not defined (VEI=ND). The grey dashed lines correspond to the contours of constant seismic energy density e (in J/m^3) varying from 0.0001 to 100 J/m^3. The red dash line corresponds to e = 0.01 J/m^3 crossing the three black lines of Index = 10 and the green dash line corresponds to e = 10 J/m^3 crossing the three black lines of Index = 1. (For interpretation of the references to color in this figure legend, the reader is referred to the web version of this article.)

to the large phreatic eruption on 18 September 1959 (Blot, 1981). If this eruption is effectively due to this earthquake, then the triggering has a dynamic origin (because of the large index of 26.8, much larger than 10) and not a static one. Similarly, if the 13 November 2005 M4.8 earthquake, located at 146 km of Lopevi volcano (index of 63.7), may have enhanced its thermal anomaly on 19 November 2005 (Delle Donne et al., 2010), it is due to dynamic triggering and not to static triggering. The third one is the 16 July 1998 M7 earthquake, located at 652 km of Lopevi (index of 22.6). The earthquakes corresponding to Table 1 are plotted in Fig. 5 for each of the main volcanoes. It is very difficult to prove such triggering effect of far-field earthquakes without modelling the dynamic waves at the volcano and showing that the corresponding dynamic stress change is sufficient to have an influence on the volcanic activity. Only a few cases have been modelled for some worldwide volcanoes (Walter et al., 2009; Prejean and Hill, 2018; Bell et al., 2021).

6. Discussion

6.1. *Vanuatu volcanic activity is mainly triggered by near-field distance earthquakes*

Of the 69 pairs (triggering earthquake, volcanic activity) analyzed, 55 cases (~80%) had a potential triggering index ≤10 (Table 1, Fig. 5). This suggests that 80% of the eruptions at the Vanuatu volcanoes listed in Table 1 were preceded by at least one near-field earthquake. However, this finding does not mean that every near-field earthquake will necessarily trigger a volcanic eruption, as the volcano must already be in a state close to eruption for this to happen (Marzocchi et al., 2002). If a volcano is not about to erupt, even a strong near-field earthquake may not lead to an eruption. For example, the great M_w9.5 Chilean earthquake of 1960 triggered eruptions at only a few volcanoes, not all (Barrientos, 1994). In our study, we compile a catalogue of 22,079 earthquakes with magnitudes >5.5 from the USGS catalogue in a large region (between 0° and 34°S of latitude, −180° and 180° of longitude) encompasing Vanuatu, over the period from 1905 to 2022. For each earthquake, we calculate the potential triggering index at each of Vanuatu's eight volcanoes (Ambae (Aoba), Ambrym, Epi, Gaua, Kuwae, Lopevi, Suretamatai, and Yasur). Only 1712 of these earthquakes (~8%) are located in near field distances of the Vanuatu's volcanoes (index ≤10), among which only 65 (4%) actually lead to 69 eruptions (Table 1). Hence, while there is a high occurrence of earthquakes along the Vanuatu subduction, only a small fraction results in volcanic eruptions.

This information alone does not allow us to statistically exclude the possibility that the potentially triggering earthquakes may have preceded accidental eruptions. To evaluate this point, we will use the method proposed in Sawi and Manga (2018), which is based on a Monte Carlo method. We want to statistically quantify the percentage of earthquakes that occur immediately before eruptions for each active volcano in Vanuatu by varying only the occurrence time of earthquakes extracted from the 1712 earthquakes with the triggering index ≤10 corresponding to each volcano, and after 1964 to have a complete catalogue (the year 1964 is the one chosen by Sawi and Manga, 2018 as almost complete for both the earthquake and eruption catalogues). We randomly generate 1000 trials of earthquake dates corresponding to each volcano, with a maximum time lag equal to that observed in the data (195 days for Ambae, 171 days for Ambrym, 130 days for Mount Garet, and 150 days for Lopevi). For the cases of Ambae, Ambrym, Mount Garet, and Lopevi, we have 772, 983, 989, and 983 trials out of 1000 random trials where the percentage is lower than the percentage observed in this study, then we can reject the possibility of an earthquake occurring before an eruption by chance with 77.2%, 98.3%, 98.9% and 98.3% confidence, respectively. These good results may be due to the fact that the number of potential triggering earthquakes is very small compared with the total number of the regional earthquakes, and only a small proportion of these actually trigger an eruption, and to the very small number of eruptions.

Most (~80%) of the volcanic activities of Table 1 corresponds to near-field earthquake-volcano distances (Fig. 5). This means that the volcanoes have experienced mainly static, and, in lesser extent, dynamic stress changes, generated by the passage of near-field (including the static displacement field) and far-field seismic waves. We include the influence of the far-field seismic waves because as mentioned before they also act at near-field distances, with an action difficult to separate from the near-field waves as both co-exist.

There are no data points in the domain of M = 6–8 and distances <10 km (Fig. 5). This may be due to the small data set we have, but also due to the distance of the earthquakes that mainly come from the subduction, so rather far from the volcanoes (at least 10 km). For example, the 1965 swarm earthquakes that may have triggered the Mount Garet volcano occurred 142 to 202 km away. These distances are too far to consider the earthquakes to be of volcanic origin. In contrast, earthquakes that occurred close to a volcano (distance ≤ ~10 km) must be treated with caution, as they might be of volcanic origin and associated with magma intrusion and are not directly related to subduction earthquakes. However, even if these earthquakes are of volcanic origin, they can alter the local stress tensor and potentially contribute to an eruption through an earthquake-volcanic activity feedback process, as shown for example at Mauna Loa volcano, Hawaii (Walter and Amelung, 2006). In our case, only six earthquakes are <10 km away (Table 1) and their magnitudes are small (between 5.1 and 5.5), suggesting a volcanic origin. Other earthquakes are at greater distances and larger magnitudes and may have a dual origin, tectonic and volcanic. For example, the focal mechanisms of the 16 and 17 December 2018 earthquakes at Ambrym, have both a double-couple component (suggesting a tectonic contribution) and a vertical compensated linear vector dipole (CLVD) component, suggesting magma intrusion. As these earthquakes occurred after the start of the 15 December eruption and during the final magma migration (Shreve et al., 2019), they may have been triggered by magma injection. It is often difficult to separate the two aspects (tectonic and magmatic), as a large earthquake may favor magma migration within the corresponding fault or magma may migrate within a nearby dyke (Walter and Amelung, 2006), which may trigger earthquakes (Walter and Amelung, 2006; Shreve et al., 2019). For example, the M_w5.4 earthquake on 15 December 2018, 21 km from Ambrym, is followed by the drop of the lava lake 12 h later and by magma intrusion into the SE rift zone on 17 December (Shreve et al., 2019). As there are two days between the earthquake and the magma intrusion, we can assume that the earthquake had a strong influence on the magma intrusion by changing the local stress tensor. As it is difficult to know the true origin of the very near-field earthquakes, we have kept the six earthquakes in our study (Table 1), which does not change the overall conclusion of our study, because four of them correspond to the Ambrym case, and if we remove these four earthquakes, the statistical study carried out earlier allows us to conclude that we can reject the possibility of an earthquake occurring before an eruption by chance with 98.4% confidence, instead of 98.3% with these four earthquakes. The other two earthquakes correspond to the Ambae case, and we have no significant difference when we add them.

6.2. Small time delay between earthquake and changes associated to volcanic activity

The time delay between a triggering very-near-field earthquake (with an index ≤5) and an eruption of VEI ≥ 3 varies between 0 and 124 days with an average of 62 days (if we consider the cases of the literature) (Table 1). If we consider all the cases including ours, the time delay varies between 0 and 160 days with an average of 76 days and a peak at 0–2 days (Fig. 4). Past studies showed that some geophysical properties on Vanuatu volcanoes can change almost concomitantly to the earthquake or only a few days after. Hence, the time delay is rather small, from 0 day to about 2–3 months on Vanuatu volcanoes, mostly composed by low-viscosity magmas, whereas the time delays are up to 3, 5 or even 10 years for volcanoes with high-viscosity magmas (closed or open-vent) worldwide (Carr, 1977; Marzocchi, 2002; Manga and Brodsky, 2006; Eggert and Walter, 2009; Watt et al., 2009; Sawi and Manga, 2018; Nishimura, 2017, 2021). It has been proposed that this large time-delay difference may be due to the fact that the exsolution of gas (during the passing of the seismic waves or the static extension of the volcano area) can accumulate pressure inside the magma reservoir over years for the high-viscosity magma volcanoes (see references above). However, the gas escapes almost concomitantly to the triggering earthquake on basaltic low-viscosity magma open-vent volcanoes, and a pressure increase within the magma reservoir over years is very unlikely on such volcanoes unless the vent is closed (Linde and Sacks, 1998; Hill et al., 2002; Manga and Brodsky, 2006; Walter et al., 2007; Sumita and Manga, 2008; Bonali et al., 2013; Hill and Prejean, 2015; Namiki et al., 2016).

6.3. Small geophysical changes co-seismically or soon after the triggering-earthquake

The volcanic activity can be either a clear eruption with an associated VEI or only a small volcanic unrest episode detected on geophysical data during (and/or soon after) the passage of seismic waves (Seropian et al., 2021). The changes reported after earthquakes worldwide were seen on seismic activity (Moran et al., 2004; Farías et al., 2014; Farías and Basualto, 2020; West et al., 2005), thermal anomalies (Harris and Ripepe, 2007; Delle Donne et al., 2010; Coppola et al., 2016; Hill-Butler et al., 2020), and gas flux (Cigolini et al., 2007). Part of these geophysical parameters have changed and were associated to unrests at the Vanuatu volcanoes in the literature (Table 1) and are described below.

6.3.1. Seismic changes

Changes of interferometry velocities at Yasur volcano occurred concomitantly to the 9 April 2008 M7.3 regional (80 km) earthquake (Battaglia et al., 2012). Complete disappearances or appearances of families of volcanic earthquakes with similar seismic waveforms were observed simultaneously to the 9 April 2008 M7.3 tectonic earthquake (Battaglia et al., 2016a, 2016b). At Ambrym volcano, changes of the seismic period started the same day as the 9 August 2000 M6.3 earthquake located at 64 km and lasted the following day (Carniel et al., 2003). An increase of the number of volcanic tremors has been reported at Ambrym volcano after the 4 October 2000, M6.8 earthquake and lasted a few days (3–4) (Rouland et al., 2009).

6.3.2. Gas flux changes

An increase of SO_2 flux has been observed at Ambrym volcano a few days after the two 25 March 2007, M7.1 (Vanuatu) and 1 April 2007, M8.1 (Solomon Islands) earthquakes (Table 1), located at ~500 km and ~ 1500 km from the volcano (Avouris et al., 2017; Kennedy, 2017). They explained this gas flux change by dynamic triggering. This agrees with the value of our index of 15.5 and 14.5, respectively, larger than 10, hence corresponding to far-field distances and only producing a dynamic triggering. Avouris et al. (2017) mentioned that "the combined degassing from Ambrym and Gaua volcanoes shows that SO_2 output 5 days after earthquakes consistently increased by ~1 kt per day (an approximate doubling of output)" (Kennedy, 2017).

6.3.3. Thermal anomalies

Thermal anomalies not related to eruptions and recorded by satellites have been seen soon after several earthquakes, for example after 6 days at Lopevi volcano in November 2005 and after 1.1 day in October 2002 and 2.8 days in October 2004 at Yasur volcano (Delle Donne et al., 2010, Table 1). The thermal activity at Ambrym volcano is almost continuous between 2000 and 2015, oscillating between 10 and 300 MW. But a clear outlier corresponding to the highest thermal anomaly value of 4000 MW, is recorded on 21 February 2015 due to the emplacement of a small lava flow. This thermal anomaly stopped on 23

February 2015 and return to its pre-eruptive value (Coppola et al., 2016) possibly when the surface of the lava flow had cooled down. This large thermal anomaly occurred <2 days (~ 30 h) after the 19 February 2015 M6.4 near-field earthquake, located at 20 km from the volcano, and three of its aftershocks (of magnitude 5.2, 5.4 and 5.1 that occurred the same day and located in the near-field at 23, 29 and 16 km from the volcano, respectively). The stress changes (mainly the static stress) of these four earthquakes cumulate with the mainly static stress change due to a previous large M6.8 and near-field earthquake that occurred the 23 January 2015, 28 days before, and located at a distance of 97 km (Hamling and Kilgour, 2020; Firth and Cronin, 2023; Shreve et al., 2021, Table 1). These may have additionally contributed to the effusive activity of the 2015 eruption at Ambrym (Table 1, Fig. 1). This is a case for which it is difficult to point out a single earthquake as being solely responsible of the effusive activity. It is quite possible that each of the above-mentioned earthquakes could have opened up part of the magma's future path towards the surface.

6.3.4. Lava lake level

Lava lakes rarely exhibit similar persistent behavior over time, and changes in their dynamic processes reveal deep or shallow activity, as shown by the heat flux recorded by satellite on Ambrym volcano (Coppola et al., 2016; Firth and Cronin, 2023). Magma levels within the shallow conduit can be deduced from thermal anomalies recorded at open-vent volcanoes, such as on Yasur volcano (Coppola et al., 2016; Table 1).

Hence, the response of Vanuatu volcanoes to triggering earthquakes can be expected not only with a drastic post-earthquake explosion (quantified by a large VEI $\geq$ 2) but also with more subtle non-explosive geophysical changes.

The fact that the volcanoes react shortly (<2 months) after the earthquakes show that magma involved in the associated eruption is very shallow. Thus, the earthquakes act on the shallow magma reservoir and not on the deep magma chamber, at least in the short term.

6.4. Period of apparent volcanic quiescence

Lopevi and Ambrym volcanoes experienced series of "clustered" eruptions triggered by large earthquakes in time (i.e., shortly separated in time) and long inter-eruption periods of apparent volcanic inactivity (Fig. 6). We consider these clusters as a single eruption to estimate an apparent volcanic quiescent period. These periods correspond to the time separating the last date of a cluster of eruptions and the first date of the following cluster. Fig. 6 shows a period of ~10 years for Ambrym and of ~20 years for Lopevi, reflecting their difference of structure (Lopevi is a closed-vent volcano whereas Ambrym is an open-vent volcano) and their difference of magma composition (Lopevi magma has a higher viscosity than Ambrym magma). We did not consider the 1913 eruption due to a lack of data between 1913 and 1950. Note that this recurrence time calculated for triggering earthquakes is slightly decreased if we consider all the eruptions of the clusters (Beaumais et al., 2013; Sheehan and Barclay, 2016). For example, Sheehan and Barclay (2016) found an eruptive cycle of ~4 years at Ambrym volcano whereas we considered here only large eruptions potentially triggered by earthquakes and long-period of inactivity between swarms of time-clustered eruptions, leading to an eruptive cycle of ~10 years at Ambrym. Beaumais et al. (2013) proposed an eruptive cycle of 15 to 20 years since the mid-19th century at Lopevi volcano, slightly smaller than our 20-year value. The main eruptions occurred in 1939; during the 1960–65 period (Williams and Curtis, 1964; Warden, 1967), in 1980, 1998 (Beaumais et al., 2013), and since 2000 with intermittent eruptions especially in 2003 and 2008 (Handley et al., 2008; Beaumais et al., 2013). The penultimate eruption of this cycle was seen with thermal anomalies in April 2007 (Coppola et al., 2016). The last eruption occurred in March 2008 that produced a high-level eruptive column. Surprisingly, this was not seen by thermal anomalies perhaps due to cloud cover or/and the rapid drift of ashes within the nearby sea. Since March 2008 and up to the time of this writing (May 2024), no new eruption is reported on Lopevi.

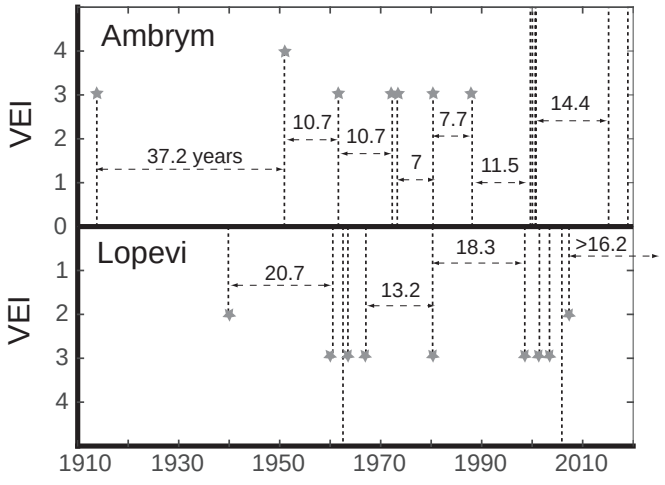

Fig. 6. Alternance of activity, following a tectonic triggering earthquake, at the two nearby volcanoes Ambrym and Lopevi separated of ~35 km. Vertical lines without stars correspond to non-explosive activity like lava flows (see text for more details).

The last large eruption (VEI $\geq$ 3) at Lopevi occurring in March 2008, Lopevi volcano may have reached the end of its quiescence period of about 15–20 years. Thus, a large eruption may occur at Lopevi volcano in the next future, perhaps triggered by an earthquake slightly before its due time.

6.5. Which parameter influence the eruption?

Even though the number of volcanoes at Vanuatu is too small to perform robust statistics, we studied the effect of open- or closed vent systems, and the VEI by plotting these parameters in the distance-magnitude plot (Fig. 7). The VEI is represented by different colors and size of the symbols and closed-vent volcanoes are represented by symbols with black circles around the color circles, whereas open-vent volcanoes have no black circles. The strongest eruptions (VEI = 3 and 4) correspond to volcanoes located in the near-field (index $\leq$10), except 3 cases. About 54% of the triggering cases correspond to closed-vent volcanoes. Note that the past activity of the open-vent Yasur volcano is underestimated because of the impossibility to define a VEI for non-strongly explosive volcanic activity. Hence, an open or closed system has no clear influence on triggering-earthquake reactivation for the Vanuatu volcanoes. But if we look only the far-field reactivations, 69% of the closed-vent volcanoes are more easily reactivated than the open-vent volcanoes. It seems that closed-vent volcanoes are more sensitive to far-field earthquake triggering than open-vent volcanoes. Note that this is an indication rather that a well-proven result given the small number of cases. Note that a bias is introduced by the fact that the VEI measure only explosions, not effusive activity. For example, Yasur is an open-vent volcano in continuous activity, and its strongest activity is not reflected by any VEI. Hence, the VEI is not a good parameter to quantify the activity of an open-vent volcano. Fig. 5 shows that the triggering effect does not clearly depend on the magma composition.

6.6. Active hydrothermal systems

Many studies have been carried out on hydrologic responses to earthquakes, such as liquefaction of the ground, the formation of new springs, the disappearance of previously active springs, changes in streams and spring discharges, changes in the properties of groundwater such as color, geochemistry, temperature and turbidity, changes in the

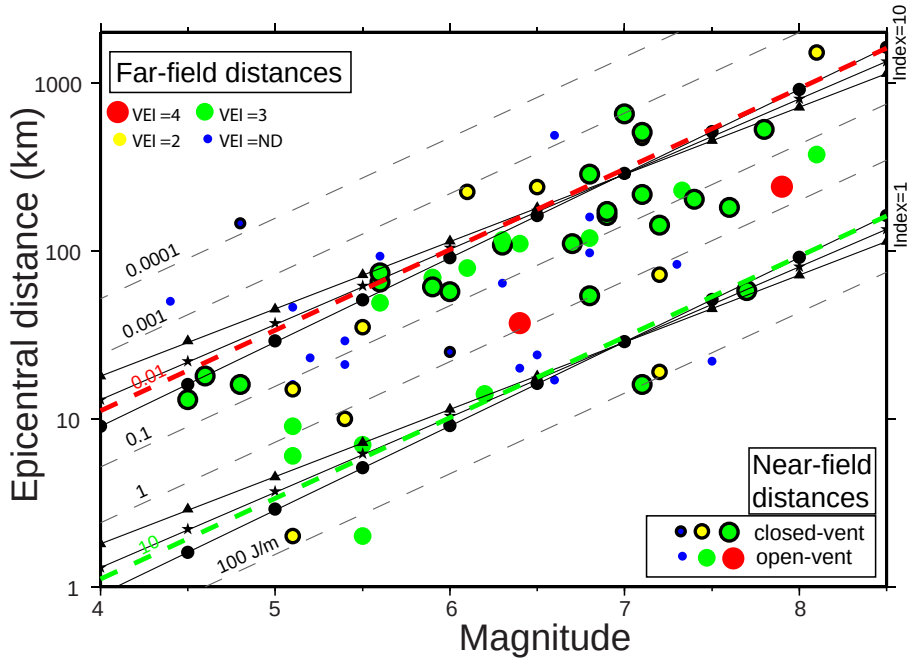

Fig. 7. Same as Fig. 5 with different symbols corresponding to the VEI and open- or closed-vent volcanoes.

water level in wells, eruptions of mud volcanoes, and changes in the eruption behavior of strato-volcanoes or in the interval between geyser eruptions (Montgomery and Manga, 2003; Wang and Manga, 2010, 2021). They show the importance of the presence of water in such earthquake triggering. What is surprising is the large amplitudes of these hydrological responses, and the great distances over which these changes occur (Wang and Manga, 2010). Wang (2007), Wang and Manga (2010, 2021) used the maximum seismic energy available in a unit volume (called the seismic energy density e) as a general metric to relate and compare the different hydrologic responses between them and with laboratory measurements and try to deduce a physical explanation to these triggering. They used an empirical relation relating e (in J/m^3), the earthquake magnitude M and the epicentral distance r (in km) initially based on strong ground motion data for southern California earthquakes (Wang, 2007):

$$log_{10}(e) = -3log_{10}(r) + 1.44M - 4.62 \quad (1)$$

No distinction is made among the different magnitude scales because this information if often not available for historical earthquakes. The epicentral distance is used because the depth of historical earthquakes is often unknown. The seismic energy density is approximately proportional to the square of the peak ground velocity (Wang et al., 2006) which in turn is proportional to the dynamic strain (e.g., Brodsky et al., 2003). Wang and Manga (2010, 2021) showed that some hydrologic changes require much greater seismic energy density while other occur under very small seismic energy density. For example, liquefaction, eruption of mud volcanoes, increases in streamflow have e-value below $\sim 10^{-1}$ J/m^3; temperature changes in hot springs have e-value below $\sim 10^{-2}$ J/m^3; most sustained groundwater changes have e-value below $\sim 10^{-3}$ J/m^3; geysers and triggered seismicity may respond to seismic energy density as small as 10^{-3} and 10^{-4} J/m^3, respectively (Wang and Manga, 2010). Recently, Wang and Manga (2021) showed that groundwater level may respond to very small values of $e < 10^{-6}$ J/m^3.

In Fig. 5, we plotted this eq. (1) for seven values of e varying from 10^{-4} to 100 J/m^3 to compare with the hydrologic responses of Wang and Manga (2010). Most of our triggering volcanic activity at Vanuatu volcanoes need seismic energy density between 10^{-2} to 10^{2} J/m^3. These values are between those found by Wang and Manga (2010) varying from $\sim 10^{-4}$ to 10^{4} J/m^3 for all hydrological responses and very similar to their value from $\sim 10^{-1}$ to 10^{2} J/m^3 for magmatic eruptions. The $e = 10^{-2}$ J/m^3 value of the seismic energy density plotted as a red dashed line in Fig. 5 corresponds to TRIGI = 10, which is the limit between far-field and near-field distances for normal, reverse and strike-slip faulting plotted as black solid lines in Fig. 5 and $e = 10$ J/m^3 plotted as a green dashed line in Fig. 5 corresponds to TRIGI = 1. Hence, values of e larger than 10^{-2} J/m^3 correspond to near-field distances, for which static stress changes can have a large influence on the magmatic volcanic responses. This value of 10^{-2} J/m^3 is different from the one of 10 J/m^3 proposed by Wang (2007) due to the difference of definition of the near-field distance as a distance equal to the rupture length (Wang, 2007). We prefer a factor of 10 for the reason we explained before. Note that Wang and Manga (2014) often defined the distances corresponding to TRIGI between 1 and 10 as intermediate field.

Based on laboratory experiments, the seismic energy density e values imply some mechanisms. Wang and Manga (2010) proposed that changes in permeability and redistribution of pore pressure can be a mechanism to explain hydrological responses. Our study at Vanuatu volcanoes suggest that this mechanism can also explain magmatic responses to earthquakes when an active hydrothermal system is present near the volcano. As most of our volcanic responses correspond to near-field observations, we propose that increase in permeability generated by the static stress changes of near-field seismic waves including the static displacement field, are the main mechanism of these changes.

Lopevi and Ambrym are the volcanoes whose volcanic activity is the most enhanced by far-field earthquakes, corresponding to 9 cases (green squares in Fig. 5), and 2 cases (red squares in Fig. 5), respectively. It has been observed on many volcanoes worldwide that after far-field earthquakes the volcanic and/or seismic activity is greatly enhanced by dynamic triggering when an active hydrothermal system is present (Hill et al., 1993, 2002; Husen et al., 2004; Moran et al., 2004; Manga and Brodsky, 2006; Prejean and Haney, 2014; Hill and Prejean, 2015; Hurwitz and Manga, 2017; Prejean and Hill, 2018; Seropian et al., 2021). These active hydrothermal systems can have visible surface manifestations, such as acidic water crater lakes, fumaroles or can be a deeper and "hidden" system, without clear surface activity (Seropian et al., 2021). The later are only detected by geophysical measurements such as on Yasur volcano (Brothelande et al., 2016).

We suggest here that the quiescence periods of ~10 and ~ 20 years

observed at Ambrym and Lopevi respectively (Fig. 5) are of the order of magnitude of the time expected to recharge an overpressure inside a sealed hydrothermal system. When magmatic fluids are injected into the hydrothermal system, they condense and vaporize the hydrothermal and/or meteoritic water. This process, which occurs at high temperatures, can induce alteration of the host rock and the formation of sulfur precipitates (Christenson et al., 2010), ultimately leading to the development of a hydrothermal seal (Stix and de Moor, 2018; Kunrat et al., 2020). When the seal is in place, an overpressure can be reached due to the accumulation of ascending mixed hydrothermal-magmatic fluids, and therefore makes the system prone to eruption. Our results indicate that the time-interval between large eruptions that have been potentially triggered by earthquakes (we discarded the other ones) is ~10 years at Ambrym volcano and is ~20 years at Lopevi volcano. We suggest that this 10–20-year period is the time necessary for the hydrothermal seal to be developed on Ambrym and Lopevi volcanoes, respectively, increasing the pressure inside the hydrothermal system. The passage of the seismic waves below Lopevi, generated by a large earthquake, may rupture the seal acting at the top of the pressurized hydrothermal system, and subsequently triggered a change of volcanic activity that can lead to eruption. Hence, we suggest the existence of an active hydrothermal system below Lopevi and Ambrym volcanoes.

At Yasur volcano, some families of similar earthquakes disappeared while others appeared after the 9 April 2008 M7.3 earthquake. The families that appeared lasted for a short time of only a few months (Battaglia et al., 2016a, 2016b) suggesting it is not a permanent process but a transient one such as due to fluid circulations. One possible explanation is the closing of some cracks, impending fluid circulation and opening of other cracks favoring fluid circulation in an active hydrothermal system. It is then reasonable to think that the significant change in the seismic waveforms observed at Yasur before and after the M7.3 earthquake may partially result from changes of permeability in the hydrothermal system, thereby changing the elastic properties of the media close to the conduit and magma reservoir and generating a change in velocity calculated by seismic coda wave interferometry (Battaglia et al., 2012).

The presence of active hydrothermal systems in most of the Vanuatu volcanoes may explain the short time reaction to the potentially triggering earthquakes. We summarized the main points of the study in Table 1.

7. Conclusion

Most (~80%) Vanuatu volcanic activity studied here is potentially triggered by near-field distance earthquakes, located at a distance ten times smaller than the characteristic rupture length of the earthquake, suggesting a large influence of static stress changes. The time-delay between the potentially triggering-earthquake and volcanic activity is between 0 day and in average ~ 2–3 months on Vanuatu volcanoes. This short time-delay at low-viscosity magma Vanuatu volcanoes is different from some of the worldwide volcanoes with high-viscosity magma, for which the time-delay can be much larger, up to several years. The reaction of Vanuatu volcanoes to potentially triggering-earthquakes seems independent of closed- or open-vent systems because Lopevi volcano (closed-vent) and Ambrym volcano (open-vent) have the same number (nine) of eruptions being triggered by an earthquake, between 1913 and 2018. The common feature of potentially triggering-earthquake sensitivity in Vanuatu volcanoes (Ambae, Ambrym, Garet, Lopevi and Yasur) may be the existence of an active hydrothermal system. In particular, the high-level dynamic earthquake triggering to far-field earthquakes observed at Lopevi suggests that this volcano has a particularly active hydrothermal system. The seismic energy density values varying between 10^{-2} to 100 J/m^3 of the seismic waves generated by the triggering earthquakes suggest a change of the permeability of the hydrothermal system of the Vanuatu volcanoes, by opening/closing of cracks, generated increase of the inner magma reservoir pressure, and leading to an eruption. The open or closed-vent character seems to poorly influence the triggering-earthquake effects. The differences of behavior of the Vanuatu volcanoes after potentially triggering earthquakes are important in term of volcanic hazards.

CRediT authorship contribution statement

D. Legrand: Writing – review & editing, Writing – original draft, Visualization, Supervision, Methodology, Investigation, Formal analysis, Data curation, Conceptualization. **P. Bani:** Writing – review & editing, Writing – original draft, Visualization, Supervision. **S. Vergniolle:** Writing – review & editing, Writing – original draft, Supervision, Methodology.

Declaration of competing interest

The authors have no conflict of interests.

Data availability

No data was used for the research described in the article.

Acknowledgments

D. L. has been supported by UNAM and the PASPA-DGAPA, UNAM program, as a sabbatical stay at Institut de Recherche et de Développement, Nouméa, Nouvelle Calédonie from 1 April to 30 September 2023. S.V. thanks her funding sources to work on the volcanoes in Vanuatu, such as the internal funding from Institut de Physique du Globe de Paris (BQR, 2018), ANR-CATELL "ARC VANUATU", and the Tellus Program of CNRS/INSU (2018, 2020).

References

Aki, K., Richards, P., 2002. Quantative Seismology, Second edition. University Science Books, p. 700.

Allard, P., Aiuppa, A., Bani, P., Métrich, N., Bertagnini, A., Gauthier, P.J., Shinohara, H., Sawyer, G., Parello, F., Bagnato, E., Pelletier, B., Garaebiti, E., 2016. Prodigious emission rates and magma degassing budget of major, trace and radioactive volatile species from Ambrym basaltic volcano, Vanuatu island Arc. J. Volcanol. Geotherm. Res. 322, 119–143. https://doi.org/10.1016/j.jvolgeores.2015.10.004.

Allen, S.R., 2005. Complex spatter- and pumice-rich pyroclastic deposits from an andesitic caldera-forming eruption: the Siwi pyroclastic sequence, Tanna, Vanuatu. Bull. Volcanol. 67, 27–41. https://doi.org/10.1007/s00445-004-0358-6.

Avouris, D.M., Carn, S.A., Waite, G.P., 2017. Triggering of volcanic degassing by large earthquakes. Geology 45 (8), 715–718. https://doi.org/10.1130/G39074.1.

Baillard, C., Crawford, W.C., Ballu, V., Pelletier, B., Garaebiti, E., 2018. Tracking subducted redges through intermediate-depth seismicity in the Vanuatu subduction zone. Geolog. Soc. Am. 46 (9), 767–770. https://doi.org/10.1130/G45010.1.

Bani, P., Lardy, M., 2007. Sulfur dioxide emission rates from Yasur volcano, Vanuatu archipelago. Geophys. Res. Lett. 34, L20309 https://doi.org/10.1029/2007GL030411.

Bani, P., Oppenheimer, C., Tsanev, V.I., Carn, S.A., Cronin, S.J., Crimp, R., Calkins, J.A., Charley, D., Lardy, M., Roberts, T.R., 2009. Surge in Sulphur and halogen degassing from Ambrym volcano. Vanuatu Bull. Volcanol. 71 (10), 1159–1168. https://doi.org/10.1007/s00445-009-0293-7.

Bani, P., Oppenheimer, C., Varekamp, J.C., Quinou, T., Lardy, M., Carn, S., 2009a. Remarkable geochemical changes and degassing at Voui crater lake, Ambae volcano, Vanuatu. J. Volcanol. Geotherm. Res. 188, 347–357. https://doi.org/10.1016/j.jvolgeores.2009.09.018.

Bani, P., Join, J.L., Cronin, S.J., Lardy, M., Rouet, I., Garaebiti, E., 2009b. Characteristics of the summit lakes of Ambae volcano and their potential for generating lahars. Nat. Hazards Earth Syst. Sci. 9 (4), 1471–1478.

Bani, P., Oppenheimer, C., Allard, P., Shinohara, H., Tsanev, V., Carn, S., Lardy, M., Garaebiti, E., 2012. First estimate of volcanic SO2 budget for Vanuatu island arc. J. Volcanol. Geotherm. Res. 211–212, 36–46. https://doi.org/10.1016/j.jvolgeores.2011.10.005.

Bani, P., Boudon, G., Balcone-Boissard, H., Delmelle, P., Quiniou, T., Lefèvre, J., Garaebiti, E., Hiroshi, S., Lardy, M., 2016. The 2009–2010 eruption of Gaua volcano (Vanuatu archipelago): Eruptive dynamics and unsuspected strong halogens source. J. Volcanol. Geotherm. Res. 322, 63–75.

Barrientos, S.E., 1994. Large thrust earthquakes and volcanic eruptions. PAGEOPH 142 (1), 225–237. https://doi.org/10.1007/BF00875972.

Battaglia, J., Métaxian, J.P., Garaebiti, E., 2012. Earthquake-volcano interaction imaged by coda wave interferometry. Geophys. Res. Lett. 39, 11. https://doi.org/10.1029/2012GL052003.s.

Battaglia, J., Métaxian, J.P., Garaebiti, E., 2016a. Families of similar events and modes of oscillation of the conduit at Yasur volcano (Vanuatu). J. Volcanol. Geotherm. Res. 322, 196–211. https://doi.org/10.1016/j.jvolgeores.2015.11.003.

Battaglia, J., Métaxian, J.-P., Garaebiti, E., 2016b. Short term precursors of Strombolian explosions at Yasur volcano (Vanuatu). Geophys. Res. Lett. 43, 1–6. https://doi.org/10.1002/2016gl067823.

Beaumais, A., Chazot, G., Dosso, L., Bertrand, H., 2013. Temporal source evolution and crustal contamination at Lopevi Volcano, Vanuatu Island Arc. J. Volcanol. Geotherm. Res. 264, 72–84. https://doi.org/10.1016/j.jvolgeores.2013.07.005.

Bebbington, M.S., Marzocchi, W., 2011. Stochastic models for earthquake triggering of volcanic eruptions. J. Geophys. Res. 116 (B5), B05204 https://doi.org/10.1029/2010JB008114.

Bell, A.F., Hernandez, S., McCloskey, J., Ruiz, M., LaFemina, P.C., Bean, C.J., Möllhoff, M., 2021. Dynamic earthquake triggering response tracks evolving unrest at Sierra Negra volcano, Galápagos Islands. Sci. Adv. 7, eabh0894.

Bergeot, N., Bouin, M.N., Diament, M., Pelletier, B., Régnier, M., Calmant, S., Ballu, V., 2009. Horizontal and vertical interseismic velocity fields in the Vanuatu subduction zone from GPS measurements: evidence for a Central Vanuatu locked zone. J. Geophys. Res. Solid Earth 114, B06405. https://doi.org/10.1029/2007JB005249.

Blaser, L., Kruger, F., Ohrnberger, M., Scherbaum, F., 2010. Scaling relations of earthquake source parameter estimates with special focus on subduction environment. B Seismol. Soc. 100 (6), 2914–2926. https://doi.org/10.1785/0120100111.

Blot, C., 1964. Origine profonde des séismes superficiels et des éruptions volcaniques. Publ. BCIS 23, 103–121.

Blot, C., 1965. Relations entre les séismes profonds et les éruptions volcaniques au Japon. Bull. Volcanol. XXVIII, 25–64.

Blot, C., 1981. Deep root of andesitic volcanoes: new evidence of magma generation at depth in the Benioff zone. J. Volcanol. Geotherm. Res. 10, 339–364.

Bonali, F.L., 2013. Earthquake-induced static stress change on magma pathway in promoting the 2012 Copahue eruption. Tectonophysics 608, 127–137. https://doi.org/10.1016/j.tecto.2013.10.006.

Bonali, F.L., Tibaldi, A., Corazzato, C., Tormey, D.R., Lara, L.E., 2013. Quantifying the effect of large earthquakes in promoting eruptions due to stress changes on magma pathway: the Chile case. Tectonophysics 583, 54–67. https://doi.org/10.1016/j.tecto.2012.10.025.

Boulesteix, T., Legrand, D., Taquet, N., Coppola, D., Laiolo, M., Valade, S., Massimetti, F., Caballero-Jiménez, G., Campion, R., 2022. Modulation of Popocatépetl's activity by regional and worldwide earthquakes. Bull. Volcanol. 84, 80. https://doi.org/10.1007/s00445-022-01584-2.

Brodsky, E.E., Sturtevant, B., Kanamori, H., 1998. Earthquakes, volcanoes, and rectified diffusion. J. Geophys. Res. 103, 23827–23838. https://doi.org/10.1029/98JB02130.

Brodsky, E.E., Roeloffs, E., Woodcock, D., Gall, I., Manga, M., 2003. A mechanism for sustained groundwater pressure changes induced by distant earthquakes. J. Geophys. Res. 108, 2390. https://doi.org/10.1029/2002JB002321.

Brothelande, E., Lénat, J.F., Chaput, M., Gailler, L., Finizola, A., Dumont, S., Peltier, A., Bachèlery, P., Barde-Cabusson, S., Byrdina, S., Menny, P., Colonge, J., Douillet, G.A., Letort, J., Letourneur, L., Merle, O., Di Gangi, F., Nakedau, D., Garaebiti, E., 2016. Structure and evolution of an active resurgent dome evidenced by geophysical investigations: the Yenkahe dome-Yasur volcano system (Siwi caldera, Vanuatu). J. Volcanol. Geotherm. Res. 322, 241–262.

Calmant, S., Pelletier, B., Lebellegard, P., Bevis, M., Taylor, F.W., Phillips, D.A., 2003. New insights on the tectonics along the New Hebrides subduction zone based on GPS results. J. Geophys. Res. Solid Earth 108 (B6), 2319. https://doi.org/10.1029/2001JB000644.

Campion, R., Delgado-Granados, H., Legrand, D., Taquet, N., Boulesteix, T., Pedraza-Espitía, S., Lecocq, T., 2018. Breathing and coughing: the extraordinarily high degassing of Popocatépetl volcano investigated with an SO2 camera. Front. Earth Sci. 6, 163. https://doi.org/10.3389/feart.2018.00163.

Carn, S.A., Fioletov, V.E., McLinden, C.A., Li, C., Krotkov, N.A., 2017. A decade of global volcanic SO2 emissions measured from space. Sci. Rep. 7 (1), 44095. https://doi.org/10.1038/srep44095.

Carney, J.N., McFarlane, A., 1979. Geology of Tanna, Aneityum, Futuna and Aniwa. New Hebrides Govern. Geol. Surv. 5–29.

Carniel, R., Di Cecca, M., Rouland, D., 2003. Ambrym, Vanuatu (July–August 2000): spectral and dynamical transitions on the hours-todays timescale. J. Volcanol. Geotherm. Res. 128 (1–3), 1–13. https://doi.org/10.1016/S0377-0273(03)00243-9.

Carr, M.J., 1977. Volcanic activity and great earthquakes at convergent plate margins. Science 197 (4304), 655–657. https://doi.org/10.1126/science.197.4304.655.

Chesley, C., LaFemina, P.C., Puskas, C., Kobayashi, D., 2012. The 1707 Mw8.7 Hoei earthquake triggered the largest historical eruption of Mt Fuji. Geophys. Res. Lett. 39 (24) https://doi.org/10.1029/2012GL053868.

Christenson, B.W., Reyes, A.G., Young, R., Moebis, A., Sherburn, S., Cole-Baker, J., Britten, K., 2010. Cyclic processes and factors leading to phreatic eruption events: insights from the 25 September 2007 eruption through Ruapehu crater lake, New Zealand. J. Volcanol. Geotherm. Res. 191, 15–32. https://doi.org/10.1016/j.jvolgeores.2010.01.008.

Cigolini, C., Laiolo, M., Coppola, D., 2007. Earthquake–volcano interactions detected from radon degassing at Stromboli (Italy). Earth Planet. Sci. Lett. 257 (3–4), 511–525. https://doi.org/10.1016/j.epsl.2007.03.022.

Collot, J.Y., Daniel, J., Burne, R.V., 1985. Recent tectonics associated with the subduction collision of the d'Entrecasteaux zone in the Central New Hebrides. Tectonophysics 112 (1–4), 325–356.

Coppola, D., Laiolo, M., Cigolini, C., Delle Donne, D., Ripepe, M., 2016. Enhanced volcanic hot-spot detection using MODIS IR data:results from the MIROVA system. Geol. Soc. London. Special Pub. 426 (1), 181–205. https://doi.org/10.1144/SP426.5.

Coppola, D., Macedo, O., Ramos, D., Finizola, A., Delle Donne, D., del Carpio, J., White, R., McCausland, W., Centeno, R., Rivera, M., Apaza, F., Ccallata, B., Chilo, W., Cigolini, C., Laiolo, M., Lazarte, I., Machaca, R., Masias, P., Ortega, M., Puma, N., Taipe, E., 2015. Magma extrusion during the Ubinas 2013-2014 eruptive crisis based on satellite thermal imaging (MIROVA) and ground-based monitoring. J. Volcanol. Geotherm. Res. 302, 199–210. https://doi.org/10.1016/j.jvolgeores.2015.07.005.

Coppola, D., Laiolo, M., Cigolini, C., 2016. Fifteen years of thermal activity at Vanuatu's volcanoes (2000-2015) revealed by MIROVA. J. Volcanol. Geotherm. Res. 322, 6–10. https://doi.org/10.1016/j.jvolgeores.2015.11.005.

Cummins, P.R., 1997. Earthquake near field and W phase observations at teleseismic distances. Geophys. Res. Lett. 24 (22), 2857–2860.

Daniel, J., Katz, H.R., 1981. D'Entrecasteaux, zone, trench and western chain of the Central New Hebrides island arc: their significance and tectonic relationship. Geo-Mar. Lett. 1, 213–219.

Darwin, C.R., 1840. On the connexion of certain volcanic phenomena in South America; and on the formation of mountain chains and volcanos, as the effect of the same power by which continents are elevated. Trans. Roy. Soc. London 5, 601–632.

De la Cruz-Reyna, S., Tárraga, M., Ortiz, R., Martínez-Bringas, A., 2010. Tectonic earthquakes triggering volcanic seismicity and eruptions. Case studies at Tungurahua and Popocatépetl volcanoes. J. Volcanol. Geotherm. Res. 193 (1–2), 37–48. https://doi.org/10.1016/j.jvolgeores.2010.03.005.

Delle Donne, D., Harris, A.J.L., Ripepe, M., Wright, R., 2010. Earthquake-induced thermal anomalies at active volcanoes. Geology 38 (9), 771–774. https://doi.org/10.1130/G30984.1.

Díez, M., La Femina, P., Connor, C., Strauch, W., Tenorio, V., 2005. Evidence for static stress changes triggering the 1999 eruption of Cerro Negro Volcano, Nicaragua and regional aftershock sequences. Geophys. Res. Lett. 32, 1–4.

Eggert, S., Walter, T.R., 2009. Volcanic activity before and after large tectonic earthquakes: observations and statistical significance. Tectonophysics 471 (1–2), 14–26. https://doi.org/10.1016/j.tecto.2008.10.003.

Engdahl, E.R., Villaseñor, A., 2002. Global Seismicity 1900-1999. Chapter 41 of International handbook of earthquake and engineering seismology 81A, pp. 665–690.

Farías, C., Basualto, D., 2020. Reactivating and calming volcanoes: the 2015 Mw8.3 Illapel Megathrust strike. Geophys. Res. Lett. 47 (16) https://doi.org/10.1029/2020GL087738.

Farías, C., Lupi, M., Fuchs, F., Miller, S., 2014. Seismic activity of the Nevados de Chillán volcanic complex after the 2010 Mw8.8 Maule, Chile, earthquake. J. Volcanol. Geotherm. Res. 283, 116–126.

Firth, C., Cronin, S., 2023. Life-cycles of a lava lake: Ambrym volcano, Vanuatu. J. Volcanol. Geotherm. Res. 434 https://doi.org/10.1016/j.jvolgeores.2022.107742.

Firth, C.W., Handley, H.K., Cronin, S.J., Turner, S.P., 2014. The eruptive history and chemical stratigraphy of a steady-state volcano: Yasur, Vanuatu. Bull. Volcanol. 76, 837. https://doi.org/10.1007/s00445-014-0837-3.

Gudmundsson, G., Saemundsson, K., 1980. Statistical Analysis of Damaging Earthquakes and Volcanic Eruptions in Iceland from 1550-1978. J. Geophys. 47, 99–109.

Hamling, I.J., Kilgour, G., 2020. Goldilocks conditions required for earthquakes to trigger basaltic eruptions: evidence from the 2015 Ambrym eruption. Sci. Adv. 6 (14), eaaz5261 https://doi.org/10.1126/sciadv.aaz5261.

Handley, H., Turner, S., Smith, I., Stewart, R., Cronin, S., 2008. Rapid timescales of differentiation and evidence for crustal contamination at intra-oceanic arcs: geochemical and U–Th–Ra–Sr–Nd isotopic constraints from Lopevi Volcano, Vanuatu, SW Pacific. Earth Planet. Sci. Lett. 273 (1–2), 184–194.

Harris, A.J.L., Ripepe, M., 2007. Regional earthquake as a trigger for enhanced volcanic activity: evidence from MODIS thermal data. Geophys. Res. Lett. 34 (2), L02304 https://doi.org/10.1029/2006GL028251.

Heap, M., Kennedy, B., 2016. Exploring the scale-dependent permeability of fractured andesite. Earth Planet. Sci. Lett. 447, 139–150. https://doi.org/10.1016/j.epsl.2016.05.004.

Hill, D., Prejean, S., 2015. Dynamic triggering. In: Schubert, G. (Ed.), Treatise on Geophysics. Elsevier B.V, pp. 274–304.

Hill, D.P., Reasenberg, P.A., Michael, A., Arabaz, W.J., Beroza, G., Brumbaugh, D., Brune, J.N., Castro, R., Davis, S., dePolo, D., Ellsworth, W.L., Gomberg, J., Harmsen, S., House, L., Jackson, S.M., Johnston, M.J.S., Jones, L., Keller, R., Malone, S., Munguia, L., Nava, S., Pechmann, J.C., Sanford, A., Simpson, R.W., Smith, R.B., Stark, M., Stickney, M., Vidal, A., Walter, S., Wong, V., Zollweg, J., 1993. Seismicity remotely triggered by the magnitude 73 Landers, California, earthquake. Science 260 (5114), 1617–1623. https://doi.org/10.1126/science.260.5114.1617.

Hill, D.P., Pollitz, F., Newhall, C., 2002. Earthquake–volcano interactions. Phys. Today 55 (11), 41–47. https://doi.org/10.1063/1.1535006.

Hill-Butler, C., Blackett, M., Wright, R., Trodd, N., 2020. The co-incidence of earthquakes and volcanoes: assessing global volcanic radiant flux responses to earthquakes in the 21st century. J. Volcanol. Geotherm. Res. 393, 106770.

Hurwitz, S., Manga, M., 2017. The fascinating and complex dynamics of geyser eruptions. Annu. Rev. Earth Planet. Sci. 45, 31–59.

Husen, S., Taylor, R., Smith, R., Healser, H., 2004. Changes in geyser eruption behavior and remotely triggered seismicity in Yellowstone National Park produced by the 2002 M 7.9 Delani fault earthquake, Alaska. Geology 32, 537–540.

Iezzi, A.M., Fee, D., Kim, K., Jolly, A.D., Matoza, R.S., 2019. Three-Dimensional acoustic multipole waveform inversion at Yasur Volcano, Vanuatu. J. Geophys. Res. Solid Earth 124, 8679–8703. https://doi.org/10.1029/2018JB017073.

Ioualalen, M., Pelletier, B., Solis Gordillo, G., 2017. Investigating the March 28th 1875 and the September 20th 1920 earthquakes/tsunamis of the Southern Vanuatu arc, offshore Loyalty Islands, New Caledonia. Tectonophysics 709, 20–38. https://doi.org/10.1016/j.tecto.2017.05.006.

Johnson, L., 1974. Green's function for Lamb's problem. Geophys. J. R. Astron. Soc. 37, 99–131.

Kennedy, B., 2017. What effects do earthquakes have on volcanoes? Geology 45, 765–766.

Kilb, D., Gomberg, J., Bodin, P., 2002. Aftershock triggering by complete Coulomb stress changes. J. Geophys. Res. 107 https://doi.org/10.1029/2001JB000202.

King, C.-Y., Azuma, S., Igarashi, G., Ohno, M., Saito, H., Wakita, H., 1999. Earthquake-related water-level changes at 16 closely clustered wells in Tono, Central Japan. J. Geophys. Res. 104 (13), 073–082.

Kunrat, S., Bani, P., Haerani, N., et al., 2020. First gas and thermal measurements at the frequently erupting Gamalama volcano (Indonesia) reveal a hydrothermally dominated magmatic system. J. Volcanol. Geotherm. Res. 407, 107096 https://doi.org/10.1016/j.jvolgeores.2020.107096.

Kuribayashi, E., Tatsuoka, F., 1975. Brief review of liquefaction during earthquakes in Japan. Soils Found. 15, 81–92.

Lagabrielle, Y., Pelletier, B., Cabioch, G., Régnier, M., Calmant, S., 2003. Coseismic and long-term vertical displacement due to back arc shortening, central Vanuatu: offshore and onshore data following the Mw 7.5, 26 November 1999 Ambrym earthquake. J. Geophys. Res. 108 (B11), 2519. https://doi.org/10.1029/2002JB002083.

Lages, J., Moussallam, Y., Bani, P., Peters, N., Aiuppa, A., Bitetto, M., Giudice, G., 2020. First In-Situ Measurements of Plume Chemistry at Mount Garet Volcano, Island of Gaua (Vanuatu). Appl. Sci. 10, 7293. https://doi.org/10.3390/app10207293.

Latter, J., 1971. The interdependence of seismic and volcanic phenomena: some time-space relationships in seismicity and volcanism. Bull. Volcanol. 35, 1–16.

Lay, T., Wallace, T., 1995. Modern Global Seismology,. Academic, p. 521.

Legrand, D., 2022. Which earthquake can trigger a volcanic eruption? J. Volcanol. Geotherm. Res. 432, 107698 https://doi.org/10.1016/j.jvolgeores.2022.107698.

Legrand, D., Delouis, B., 1999. Determination of the fault plane using single near field seismic station with a finite-dimension of source model. Geophys. J. Int. 138, 801–808.

Legrand, D., Rouland, D., Frogneux, M., Carniel, R., Charley, D., Roult, G., Robin, C., 2005. Interpretation of very long period tremors at Ambrym volcano, Vanuatu, as quasi-static displacement field related to two distinct magmatic sources. Geophys. Res. Lett. 32, L06314. https://doi.org/10.1029/2004GL021968.

Linde, A.T., Sacks, I.S., 1998. Triggering of volcanic eruptions. Nature 395 (6705), 888–890. https://doi.org/10.1038/27650.

Louat, R., Pelletier, B., 1989. Seismotectonics and present day relative plate motions in the New Hebrides–North Fiji Basin region. Tectonophysics 167, 41–55.

MacFarlane, A., Carney, J., Crawford, A., Greene, H., 1988. Vanuatu: A reviewof the onshore geology. In: Greene, H.G., Wong, F.L. (Eds.), Geology and Offshore Resources of Pacific Islands Arcs-Vanuatu Region Earth Sci Ser 8. Circum Pac Counc for Energy and Miner Res Houston, Tex, pp. 45–91.

MacGregor, A., 1949. Prediction in relation to seismo-volcanic phenomena in the caribbean volcanic arc. Bull. Volcanol. 8, 69–86.

Mallick, D., Ash, R., 1975. Geology of the Southern Banks Islands. New Hebrides Condomin. Geol. Surv. 33.

Manga, M., 2001. Origin of postseismic streamflow changes inferred from baseflow recession and magnitude-distance relations. Geophys. Res. Lett. 28, 2133–2136.

Manga, M., Brodsky, E., 2006. Seismic triggering of eruptions in the far field: volcanoes and geysers. Annu. Rev. Earth Planet. Sci. 34 (1), 263–291. https://doi.org/10.1146/annurev.earth.34.031405.125125.

Manga, M., Wang, C.-Y., 2007. Earthquake hydrology. In: Kanamori, H. (Ed.), Earthquake Seismology, Ch. 4.10. Elsevier, Amsterdam, pp. 293–320. Vol. 4 of Treatise on Geophysics.

Marzocchi, W., 2002. Remote seismic influence on large explosive eruptions. J. Geophys. Res. 107 (B1) https://doi.org/10.1029/2001JB000307.

Marzocchi, W., Casarotti, E., Piersanti, A., 1993. The tectonic setting of Mount Vesuvius and the correlation between its eruptions and the earthquakes of the Southern Apennines. J. Volcanol. Geotherm. Res. 58, 27–41. https://doi.org/10.1016/0377-0273(93)90100-6.

Marzocchi, W., Casarotti, E., Piersanti, A., 2002. Modeling the stress variations induced by great earthquakes on the largest volcanic eruptions of the 20th century. J. Geophys. Res. 107 (B11), ESE, 13–1-ESE 13–8. https://doi.org/10.1029/2001JB001391.

McCall, G., LeMaitre, R., Malahoff, A., Robinson, G., Stephenson, T., 1970. The geology and geophysics of the Ambrym Caldera, New Hebrides. Bull. Volcanol. 34, 681–696.

Métrich, N., Allard, P., Aiuppa, A., Bani, P., Bertagnini, A., Shinohara, H., Parello, F., Di Muro, A., Garaebiti, E., Belhadj, O., Massare, D., 2011. Magma and volatile supply to post-collapse volcanism and block resurgence in Siwi caldera (Tanna island, Vanuatu arc). J. Petrol. 51, 603–626. https://doi.org/10.1093/petrology/egr019.

Métrich, N., Bertagnini, A., Garaebiti, E., Vergniolle, S., Bani, P., Beaumais, A., Neuville, D.R., 2016. Magma transfert and degassing budget: application to the 2009–2010 eruptive crisis of Mt Garet (Vanuatu arc). J. Volcanol. Geotherm. Res. 322, 48–62.

Mogi, K., Mochizuki, H., Kurokawa, Y., 1989. Temperature changes in an artesian spring at Usami in the Izu Peninsula (Japan) and their relation to earthquakes. Tectonophysics 159, 95–108.

Montgomery, D.R., Manga, M., 2003. Streamflow and water well responses to earthquakes. Science 300, 2047–2049.

Moran, S.C., Power, J.A., Stihler, S.D., Sanchez, J.J., Caplan-Auerbach, J., 2004. Earthquake triggering at Alaskan volcanoes following the 3 November 2002 Denali Fault Earthquake. B Seismol. Soc. 94 (6B), S300–S309. https://doi.org/10.1785/0120040608.

Moussallam, Y., Rose-Koga, E.F., Koga, K.T., Médard, E., Bani, P., Devidal, J.L., Tari, D., 2019. Fast ascent rate during the 2017–2018 Plinian eruption of Ambae (Aoba) volcano: a petrological investigation. Contrib. Mineral. Petrol. 174, 90. https://doi.org/10.1007/s00410-019-1625-z.

Moussallam, Y., Medard, E., Georgeais, G., Rose-Koga, E.F., Koga, K.T., Pelletier, B., Bani, P., Shreve, T.L., Grandin, R., Boichu, M., Tari, D., Peters, N., 2021. How to turn off a lava lake? A petrological investigation of the 2018 intra-caldera and submarine eruptions of Ambrym volcano. Bull. Volcanol. 83, 36. https://doi.org/10.1007/s00445-021-01455-2.

Nairn, I.A., Scott, B.J., Giggenbach, W.F., 1988. Yasur volcano investigations, Vanuatu. N. Z. Geol. Surv. Rep. Geol. 134, 74.

Nakamura, K., 1975a. Volcano structure and possible mechanical correlation between volcanic eruptions and earthquakes. Bull. Volcanol. Soc. Jap. 20, 229–240.

Nakamura, K., 1975b. Volcanic eruption caused by squeeze up of magma due to compressive tectonic stress. Bull. Volcanol. Soc. Jap. 20 (2), 116.

Namiki, A., Rivalta, E., Woith, H., Walter, T.R., 2016. Sloshing of a bubbly magma reservoir as a mechanism of triggered eruptions. J. Volcanol. Geotherm. Res. 320, 156–171. https://doi.org/10.1016/j.jvolgeores.2016.03.010.

Németh, K., Cronin, S.J., 2009. Phreatomagmatic volcanic hazards where rift-systems meet the sea, a study from Ambae Island, Vanuatu. J. Volcanol. Geotherm. Res. 180, 246–258. https://doi.org/10.1016/j.jvolgeores.2008.08.011.

Nercessian, A., Hirn, A., Sapin, M., 1991. A correlation between earthquakes and eruptive phases at Mt Etna: an example and past occurrences. Geophys. J. Int. 105, 131–138.

Nishimura, T., 2017. Triggering of volcanic eruptions by large earthquakes: triggering of volcanic eruptions. Geophys. Res. Lett. 44 (15), 7750–7756. https://doi.org/10.1002/2017GL074579.

Nishimura, T., 2021. Volcanic eruptions are triggered in static dilatational strain fields generated by large earthquakes. Sci. Rep. 11, 17235. https://doi.org/10.1038/s41598-021-96756-z.

Park, I., Jolly, A., Matoza, R., Kennedy, B., Kilgour, G., Johnson, R., Garaebiti, E., Cevuard, S., 2021. Seismo-acoustic characterisation of the 2018 Ambae (Manaro Voui) eruption, Vanuatu. Bull. Volcanol. 83, 60. https://doi.org/10.1007/s00445-021-01474-z.

Peate, D.W., Pearce, J.A., Hawkesworth, C.J., Colley, H., Edwards, C.M.H., Hirose, K., 1997. Geochemical variations in Vanuatu Arc lavas: the role of subducted material and a variable mantle wedge composition. J. Petrol. 38 (10), 1331–1358.

Pelletier, B., Calmant, S., Pillet, R., 1998. Current tectonics of the Tonga–New Hebrides region. Earth Planet. Sci. Lett. 164, 263–276.

Polacci, M., Baker, D.R., La Rue, A., Mancini, L., Allard, P., 2012. Degassing behaviour of vesiculated basaltic magmas: an example from Ambrym volcano, Vanuatu Arc. J. Volcanol. Geotherm. Res. 233-234, 55–64.

Prejean, S.G., Haney, M.M., 2014. Shaking up volcanoes. Science 345 (6192), 39. https://doi.org/10.1126/science.1256196.

Prejean, S.G., Hill, D.P., 2018. The influence of tectonic environment on dynamic earthquake triggering: a review and case study on Alaskan volcanoes. Tectonophysics 745, 293–304. https://doi.org/10.1016/j.tecto.2018.08.007.

Priam, R., 1964. Une nouvelle éruption du volcan de Lopevi (Nouvelles-Hébrides) et son analogie sismique avec les éruptions précédentes. Boll. Volc. 27, 341–345.

Pritchard, M.E., Jay, J.A., Aron, F., Henderson, S.T., Lara, L.E., 2013. Subsidence at southern Andes volcanoes induced by the 2010 Maule. Chile Earthquake Nat. Geosci. 6 (8), 632–636. https://doi.org/10.1038/ngeo1855.

Pritchard, M.E., Henderson, S.T., Jay, J.A., Soler, V., Krzesni, D.A., Button, N.E., Welch, M.D., Semple, A.G., Glass, B., Sunagua, M., Minaya, E., Amigo, A., Clavero, J., 2014. Reconnaissance earthquake studies at nine volcanic areas of the Central Andes with coincident satellite thermal and InSAR observations. J. Volcanol. Geotherm. Res. 280, 90–103. https://doi.org/10.1016/j.jvolgeores.2014.05.004.

Radebaugh, J., Lopes, R.M., Howell, R.D., Lorenz, R.D., Turtle, E.P., 2016. Eruptive behavior of the Marum/Mbwelesu lava lake, Vanuatu and comparisons with lava lakes on Earth and Io. J. Volcanol. Geotherm. Res. Spec. Iss. Understand. Volcan. Vanuatu Arc 322, 105–118. https://doi.org/10.1016/j.jvolgeores.2016.03.019.

Rikitake, T., Sato, R., 1989. Up-squeezing of magma under tectonic stress. J. Phys. Earth 37, 303–311.

Robin, C., Monzier, M., 1994. Volcanic Hazards in Vanuatu, September. ORSTOM and Department of Geology. Mines andWater resources of the Vanuatu Gouvernement, Port Vila, Report, p. 15.

Robin, C., Eissen, J.-P., Monzier, M., 1994. Ignimbrites of basaltic andesite and andesite compositions from Tanna, New Hebrides Arc. Bull. Volcanol. 56, 10–22.

Robin, C., Monzier, M., Lardy, M., Régnier, M., Métexian, J.P., Decourt, R., Charley, D., Ruiz, M., Eissen, J.P., 1995. Increased steam emissions and seismicity in early February; evacuation preparations made, Aoba, Vanuatu. Bull. Glob. Volcanism Net. 20, 02.

Rockstroh, E., 1903. Recent earthquakes in Guatemala. Nature 67 (1734), 271. https://doi.org/10.1038/067271d0.

Roeloffs, E.A., 1998. Persistent water level changes in a well near Parkfield,California, due to local and distant earthquakes. J. Geophys.Res. 103, 869–889.

Rojstaczer, S., Wolf, S., Michel, R., 1995. Permeability enhancement in the shallow crust as a cause of earthquake-induced hydrological changes. Nature 373 (237). https://doi.org/10.1038/373237a0.

Rouland, D., Cisternas, A., Denkmann, R., Dufumier, H., Régnier, M., Lardy, M., 2001. The December 1994 seismic swarm near Aoba (AMBAE) volcano, Vanuatu, and its relationship with the volcanic processes. Tectonophysics 338, 23–44. https://doi.org/10.1016/S0040-1951(01)00074-9.

Rouland, D., Legrand, D., Zhizhin, M., Vergniolle, S., 2009. Automatic detection and discrimination of volcanic tremors and tectonic earthquakes: an application to Ambrym volcano, Vanuatu. J. Volcanol. Geotherm. Res. 181, 196–206.
Sawi, T.M., Manga, M., 2018. Revisiting short-term earthquake triggered volcanism. Bull. Volcanol. 80 (7), 57. https://doi.org/10.1007/s00445-018-1232-2.
Seropian, G., Kennedy, B.M., Walter, T.R., Ichihara, M., Jolly, A.D., 2021. A review framework of how earthquakes trigger volcanic eruptions. Nat. Commun. 12 (1), 1004. https://doi.org/10.1038/s41467-021-21166-8.
Sharp, A., Lombardo, G., Davis, P., 1981. Correlation between eruptions of Mount Etna, Sicily, and regional earthquakes as seen in historical records from 1582 a.D. Geophys. J. R. Astron. Soc. 65, 507–523.
Shearer, P., 2009. Introduction to Seismology. University of California, San Diego. Cambridge University Press.
Sheehan, F., Barclay, J., 2016. Staged storage and magma convection at Ambrym volcano, Vanuatu. J. Volcanol. Geotherm. Res. 322, 144–157. https://doi.org/10.1016/j.jvolgeores.2016.02.024.
Shreve, T., Grandin, R., Boichu, M., Garaebiti, E., Moussallam, Y., Ballu, V., Delgado, F., Leclerc, F., Vallée, M., Henriot, N., Cevuard, S., Tari, D., Lebellegard, P., Pelletier, B., 2019. From prodigious volcanic degassing to caldera subsidence and quiescence at Ambrym (Vanuatu): the influence of regional tectonics. Sci. Rep. 9, 1–13. https://doi.org/10.1038/s41598-019-55141-7.
Shreve, T., Grandin, R., Smittarello, D., Cayol, V., Pinel, V., Boichu, M., Morishita, Y., 2021. What triggers caldera ring-fault subsidence at Ambrym volcano? Insights from the 2015 dike intrusion and eruption. J. Geophys. Res. 126, e2020JB020277 https://doi.org/10.1029/2020JB020277.
Spina, L., Taddeucci, J., Cannata, A., Gresta, S., Lodato, L., Privitera, E., Scarlato, P., Gaeta, M., Gaudin, D., Palladino, D.M., 2016. Explosive volcanic activity at Mt. Yasur: a characterization of the acoustic events (9–12th July 2011). J. Volcanol. Geotherm. Res. 322, 175–183. https://doi.org/10.1016/j.jvolgeores.2015.07.027.
Stix, J., de Moor, M., 2018. Understanding and forecasting phreatic eruptions driven by magmatic degassing. Earth Planets Space 70, 83. https://doi.org/10.1186/s40623-018-0855-z.
Sumita, I., Manga, M., 2008. Suspension rheology under oscillatory shear and its geophysical implications. Earth Planet. Sci. Lett. 269, 468–477.
Takada, Y., Fukushima, Y., 2014. Volcanic subsidence triggered by megathrust earthquakes. J. Disaster Res. 9 (3), 373–380. https://doi.org/10.20965/jdr.2014.p0373.
Taylor, F.W., Bevis, M., Schutz, B., Kuang, D., Recy, J., Calmant, S., Charley, D., Regnier, M., Perin, B., Jackson, M., Reichenfeld, C., 1995. Geodetic measurements of convergence at the New Hebrides island arc indicate arc fragmentation caused by an impinging aseismic ridge. Geology 23, 1011–1014.
Tokarev, P., 1971. Forecasting volcanic eruptions from seismic data. Bull. Volcanol. 35, 243–250.
Ukawa, M., Fujita, E., Kumagai, T., 2002. Remote triggering of microearthquakes at the Iwo-jima volcano. J. Geogr. (chigaku Zasshi) 111 (2), 277–286. https://doi.org/10.5026/jgeog raphy.111.2_277.
Vergniolle, S., Métrich, N., 2016. A bird's eye view of "Understanding volcanoes in the Vanuatu arc.". J. Volcanol. Geotherm. Res. 322, 1–5. https://doi.org/10.1016/j.jvolgeores.2016.08.012.
Vergniolle, S., Métrich, N., 2022. An interpretative view of open-vent volcanoes. Bull. Volcanol. 84, 83. https://doi.org/10.1007/s00445-022-01581-5.
Vidale, J.E., Goes, S., Richards, P.G., 1995. Near-field deformation seen on distant broadband seismograms. Geophys. Res. Lett. 22 (1), 1–4. https://doi.org/10.1029/94GL02893.
Walter, T., 2007. How a tectonic earthquake may wake up volcanoes: stress transfer during the 1996 earthquake–eruption sequence at the Karymsky Volcanic Group. Kamchatka Earth Planet Sci. Lett. 264 (3–4), 347–359. https://doi.org/10.1016/j.epsl.2007.09.006.
Walter, T.R., Amelung, F., 2006. Volcano-earthquake interaction at Mauna Loa volcano, Hawaii. J. Geophys. Res. 111, B05204.
Walter, T.R., Amelung, F., 2007. Volcanic eruptions following M ≥ 9 megathrust earthquakes: implications for the Sumatra-Andaman volcanoes. Geology 35 (6), 539. https://doi.org/10.1130/G23429A.1.
Walter, T.R., Wang, R., Zimmer, M., Grosser, H., Lühr, B., Ratdomopurbo, A., 2007. Volcanic activity influenced by tectonic earthquakes: static and dynamic stress triggering at Mt. Merapi. Geophys. Res. Lett. 34 (5) https://doi.org/10.1029/2006GL028710.
Walter, T.R., Wang, R., Acocella, V., Neri, M., Grosser, H., Zschau, J., 2009. Simultaneous magma and gas eruptions at three volcanoes in southern Italy: an earthquake trigger? Geology 37 (3), 251–254. https://doi.org/10.1130/G25396A.
Wang, C.Y., 2007. Liquefaction beyond the near field. Seismol. Res. Lett. 78, 512–517. https://doi.org/10.1785/gssrl.78.5.512.
Wang, C.Y., Manga, M., 2010. Hydrologic responses to earthquakes and a general metric. Geofluids 10, 206–216.
Wang, C.Y., Manga, M., 2014. Earthquakes and water. In: Encyclopedia of Complexity and Systems Science. Springer, New-York. https://doi.org/10.1007/978-3-642-27737-5_606-1.
Wang, C.Y., Manga, M., 2021. Water and earthquakes. In: Lecture Notes in Earth System Science. Springer. https://doi.org/10.1007/978-3-030-64308-9.
Wang, C.-Y., Wong, A., Dreger, D.S., Manga, M., 2006. Liquefaction limit during earthquakes and underground explosions: Implications on ground-motion attenuation. Bull. Seismol. Soc. Am. 96, 355–363.
Warden, A., 1967. The 1963-65 eruption of Lopevi Volcano (New Hebrides). Bull. Volcanol. 30, 277–306.
Warden, A.J., 1970. Evolution of Aoba caldera volcano. New Hebrides, Bull. Volcanol. 24, 107–140.
Watt, S.F.L., Pyle, D.M., Mather, T.A., 2009. The influence of great earthquakes on volcanic eruption rate along the Chilean subduction zone. Earth Planet. Sci. Lett. 277 (3–4), 399–407. https://doi.org/10.1016/j.epsl.2008.11.005.
Wells, D.L., Coppersmith, K.J., 1994. New empirical relationships among magnitude, rupture length, rupture width, rupture area, and surface displacement. Bull. Seismol. Soc. Am. 84, 974–1002.
West, M., Sanchez, J.J., McNutt, S.R., 2005. Periodically triggered seismicity at Mount Wrangell, Alaska, after the Sumatra Earthquake. Science 308 (5725), 1144–1146. https://doi.org/10.1126/science.1112462.
Wiart, P., 1995. Impact et gestion des risques volcaniques au Vanuatu. Notes Techniques, Sciences de la Terre. In: Geologie-geophysique, 13. ORSTOM, Vanuatu, p. 80.
Williams, C.E., Curtis, R., 1964. The eruption of Lopevi Volcano, New Hebrides, July 1960. Bull. Volcanol. 27, 423–433.
Woitischek, J., Woods, A.W., Edmonds, M., Oppenheimer, C., Aiuppa, A., Pering, T.D., Ilanko, T., D'Aleo, R., Garaebiti, E., 2020. Strombolian eruptions and dynamics of magma degassing at Yasur Volcano (Vanuatu). J. Volcanol. Geotherm. Res. 398, 106869 https://doi.org/10.1016/j.jvolgeores.2020.106869.
Yamashina, K., Nakamura, K., 1978. Correlations between Tectonic Earthquakes and Volcanic activity of Izu-Oshima Volcano, Japan. J. Volcanol. Geotherm. Res. 4, 233–250.
Yokoyama, I., 1971. Volcanic eruptions triggered by tectonic earthquakes. Geophys. Bull. Hokkaido Univ. 25, 129–139. https://doi.org/10.14943/gbhu.25.129.
Zhang, S., Shi, Z., Wang, G., Zhang, Z., Guo, H., 2023. The origin of hydrological responses following earthquakes in a confined aquifer: insight from water level, flow rate, and temperature observations. Hydrol. Earth Syst. Sci. 27, 401–415. https://doi.org/10.5194/hess-27-401.